Logarithmic relaxation in glass-forming systems

W. Götze and M. Sperl
Physik Department, Technische Universität München, D-85747 Garching, Germany
(Received 27 March 2002; published 29 July 2002)

Within the mode-coupling theory for ideal glass transitions, an analysis of the correlation functions of glass-forming systems for states near higher-order glass-transition singularities is presented. It is shown that the solutions of the equations of motion can be asymptotically expanded in polynomials of the logarithm of time *t*. In leading order, a $\ln(t)$ law is obtained, and the leading corrections are given by a fourth-order polynomial. The correlators interpolate between three scenarios. First, there are surfaces in parameter space where the dominant corrections to the $\ln(t)$ law vanish, so that the logarithmic decay governs the structural relaxation process. Second, the dynamics due to the higher-order singularity can describe the initial and intermediate part of the α process thereby reducing the range of validity of von Schweidler's law and leading to strong α relaxation stretching. Third, the $\ln(t)$ law can replace the critical decay law of the β process, leading to a particularly large crossover interval between the end of the transient and the beginning of the α process. This may lead to susceptibility spectra below the band of microscopic excitations exhibiting two peaks. Typical results of the theory are demonstrated for models dealing with one and two correlation functions.

DOI: 10.1103/PhysRevE.66.011405 PACS number(s): 82.70.Dd, 61.20.Lc, 64.70.Pf

I. INTRODUCTION

Within the mode-coupling theory (MCT) for ideal glass transitions, the dynamics of an amorphous system of strongly interacting spherical particles is described by M functions of time t, $\phi_q(t)$, $q=1,2,\ldots,M$. These are autocorrelation functions of density fluctuations with wave-vector modulus q chosen from a grid of M values. The theory is based on a closed set of coupled nonlinear equations of motion for the $\phi_q(t)$. The coupling coefficients in these equations are given in terms of the equilibrium structure functions. The latter are assumed to be known smooth functions of the control parameters of the system like, e.g., the packing fraction φ [1]. The MCT equations exhibit fold bifurcations [2] at certain critical values of the control parameters, say at $\varphi=\varphi_c$, describing a transition from ergodic liquid dynamics for $\varphi<\varphi_c$ to nonergodic glass dynamics for $\varphi\geqslant\varphi_c$. The transition is accompanied by the evolution of a slow stretched dynamics that was suggested as the explanation of structural relaxation observed in glass-forming liquids. The leading-order asymptotic solutions of the equations for parameters approaching the transition provide predictions for the universal properties of glassy dynamics [3]. These predictions have been tested extensively against experimental data and molecular-dynamics simulation results [4,5]. The outcome of these tests qualifies MCT as a candidate for a theory of structural relaxation in glass-forming systems.

It was shown that schematic MCT models exhibit also higher-order bifurcation singularities like the cusp and swallowtail bifurcations. The accompanying dynamics is utterly different from that for the fold bifurcation. For example, in certain parameter regions, the leading order result reads $[\phi(t)-f]\propto-\ln(t/\tau)$ [6]. This logarithmic decay is equivalent to a susceptibility spectrum that is independent of frequency ω, $\chi''(\omega)\propto\omega^0$, or to a $1/f$-noise fluctuation spectrum. There are corrections to this leading-order result which alter qualitatively the straight $\phi(t)$ versus log$t$ lines or the plateaus of the $\chi''(\omega)$ versus $\log(\omega)$ plots. One needs to understand these corrections if one intends to get an overview of the relaxation scenarios for parameters near the higher-order bifurcation points. It is the goal of this paper to provide such understanding by construction of a general theory for the logarithmic relaxation law and its leading corrections.

For parameters at a cusp singularity of schematic $M=1$ models, the leading-order long-time decay follows the law $[\phi(t)-f]\propto 1/\ln^2 t$. This law has been embedded in a leading-order description of the dynamics near the singularities in terms of multiparameter scaling laws [7]. It was shown by Sjögren that dielectric-loss spectra for certain polymers could be interpreted by this scaling-law description [8], and further work extended his analysis [9–11]. However, it was also demonstrated that the cited decay laws at the critical points have to be complemented by their leading corrections in order to describe the numerical solutions of MCT equations within a time regime relevant for data analysis [7,12]. But, so far it has not been possible to evaluate the corrections for the mentioned scaling laws. The results of this paper will be obtained along a different route of asymptotic expansion of the MCT solutions than that followed in Ref. [7].

Logarithmic decay of correlations for glassy systems has been observed, for example, in Monte Carlo simulation results for a spin-glass model [13], for photon-correlation data from a dense colloidal suspension [14], and for optical Kerr-effect data for a van der Waals liquid [15]. But the present work is motivated by three recent discoveries. First, density correlators $\phi_q(t)$ measured by photon-correlation spectroscopy for colloids of micellar particles demonstrated logarithmic decay within time windows of two orders of magnitude in size [16]. Second, the MCT equations for a system whose structure was described by Baxter's model for sticky hard spheres exhibit cusp bifurcations [17,18]. These findings have been corroborated by a comprehensive analysis of the glass transitions of a square-well system [19]. Third, logarithmic decay extending over three decades in time was found in a molecular-dynamics simulation for a system with

an interaction given by a strong repulsion complemented by a short-ranged attraction [20]. One concludes that higher-order bifurcation singularities are not restricted to schematic models and that there are reasons to suggest the search for such singularities in colloids with short-ranged attraction. It is the aim of this paper to provide a detailed discussion of the qualitative features that are characteristic of the relaxation in systems near higher-order bifurcations. A set of general formulas will be derived which could be used as a basis for a quantitative analysis of future experiments and simulation studies.

The paper is organized as follows. In Sec. II A, the known general MCT equations for structural relaxation are formulated. Then (Sec. II B) these equations are rewritten in a form that is suited as a basis for an asymptotic solution near bifurcation singularities. Section III presents the theory for the logarithmic relaxation for MCT models dealing with a single correlator and in Sec. IV quantitative results are discussed for a cusp singularity in an $M=1$ model. Section V presents the theory for the general case and in Sec. VI further results are discussed for relaxation near a swallowtail singularity for an $M=2$ model. Section VII summarizes the findings.

II. BASIC EQUATIONS

A. The equations for structural relaxation

MCT is based on two sets of equations. The first one consists of the exact equations of motion for the M density correlators $\phi_q(t), q=1,2,\ldots,M$, derived within the Zwanzig-Mori formalism

$$\partial_t^2\phi_q(t)+\Omega_q^2\phi_q(t)+\int_0^t M_q(t-t')\partial_{t'}\phi_q(t')dt'=0. \tag{1a}$$

The initial conditions read $\phi_q(t=0)=1, \partial_t\phi_q(t=0)=0$. The positive Ω_q are characteristic frequencies and the kernels $M_q(t)$ are fluctuating-force correlators [21]. In colloidal suspensions, there are contributions to the force due to interactions of a colloid particle with the solvent particles. These fluctuate on a time scale much shorter than the one relevant for the motion of the mesoscopic colloid particles. Therefore, one can approximate the corresponding contributions to the kernel by a white-noise term, and this leads to a friction force $\nu_q\partial_t\phi_q(t), \nu_q>0$. Compared to this term, one can neglect the inertia term $\partial_t^2\phi_q(t)$. One arrives at the analog of Eq. (1a) for colloids, i.e., at an equation of motion where the underlying dynamics is Brownian rather than Newtonian:

$$\nu_q\partial_t\phi_q(t)+\Omega_q^2\phi_q(t)+\int_0^t M_q(t-t')\partial_{t'}\phi_q(t')dt'=0. \tag{1b}$$

The initial conditions are $\phi_q(t=0)=1$. The kernels are split into regular ones, $M_q^{\mathrm{reg}}(t)$, and so-called mode-coupling kernels $m_q(t)$ describing the cage effect: $M_q(t)=M_q^{\mathrm{reg}}(t)+\Omega_q^2 m_q(t)$. The regular terms describe normal liquid effects like binary collisions in conventional liquids or hydrodynamic interactions in colloids. The crucial step in the derivation of MCT is the application of Kawasaki's factorization approximation in order to express $m_q(t)$ as functionals $\mathcal{F}_q$ of the M correlators $\phi_k(t)$ called mode-coupling functionals. For simple systems, they are quadratic polynomials, whose coefficients are given in terms of the equilibrium structure functions [1,22]. The functionals depend smoothly on, say, N control parameters to be combined into a control parameter vector $V=(V_1,\ldots,V_N)$. In conventional liquids, the packing fraction and the temperature may be the control parameters. In colloids, one of the control parameters may be the attraction strength, which can be changed by modifying the solvent. Let us denote the functionals by $\mathcal{F}_q[V,\tilde{f}_k]$. For $0\leqslant|\tilde{f}_k|\leqslant 1, k=1,2,\ldots,M$, they can be written as Taylor series with non-negative coefficients. Thus, the second set of MCT equations is

$$m_q(t)=\mathcal{F}_q[V,\phi_k(t)]. \tag{2}$$

Specifying the functionals $\mathcal{F}_q$, the regular kernels $M_q^{\mathrm{reg}}(t)$, and the frequencies Ω_q or ν_q, Eq. (1a) or Eq. (1b) together with Eq. (2) are closed. In the present paper, a topologically stable singularity of Eqs. (1) and (2) will be discussed in full generality. Therefore, microscopic details are not of concern.

It will be convenient to discuss dynamics in the domain of complex frequencies $z, \mathrm{Im}\,z>0$. This can be achieved by Laplace transformation of functions of time, say $F(t)$, to functions of z denoted by $\mathcal{L}[F(t)](z)=i\int_0^\infty \exp(izt)F(t)dt$. Equations (1a) and (2) together with the initial conditions are equivalent to a fraction representation of $\phi_q(z)=\mathcal{L}[\phi_q(t)]\times(z)$ in terms of $M_q^{\mathrm{reg}}(z)=\mathcal{L}[M_q^{\mathrm{reg}}(t)](z)$ and $m_q(z)=\mathcal{L}[m_q(t)](z)$,

$$\phi_q(z)=-1/\{z-\Omega_q^2/[z+M_q^{\mathrm{reg}}(z)+\Omega_q^2 m_q(z)]\}. \tag{3a}$$

The analog for the colloid dynamics is derived from Eq. (1b):

$$\phi_q(z)=-1/\{z-\Omega_q^2/[i\nu_q+M_q^{\mathrm{reg}}(z)+\Omega_q^2 m_q(z)]\}. \tag{3b}$$

There are two possibilities for the solutions of the preceding equations. First, all long-time limits of the correlators may vanish as expected for an ergodic system. States with such control parameters V are referred to as liquids. Second, there may be nonvanishing long-time limits $f_q=\phi_q(t\to\infty), 0<f_q\leqslant 1$, as expected for nonergodic systems. States with such control parameters V are referred to as glasses, and f_q is called the glass form factor. Changing V, it may happen that there are values V^c where one changes from a liquid to a glass—these are the ideal liquid-glass transitions discussed within MCT [1]. For glass states, $\phi_q(z)$ exhibits a zero-frequency pole $\phi_q(z\to 0)\sim -f_q/z$. Because of Eq. (2), a similar statement holds for the kernel, $m_q(z\to 0)\sim -\mathcal{F}_q[V,f_k]/z$. Hence, for frequencies tending to zero, the kernel $m_q(z)$ becomes arbitrarily large compared to the term $z+M_q^{\mathrm{reg}}(z)$ or the term $i\nu_q+M_q^{\mathrm{reg}}(z)$, respectively. Because of continuity, for states with control parameters near the ones for glass states $\Omega_q^2 m_q(z)$ is also very large compared to z

$+M_q^{\mathrm{reg}}(z)$ or to $i\nu_q+M_q^{\mathrm{reg}}(z)$. Under the specified conditions, Eqs. (3a) and (3b) simplify to [3]

$$\phi_q(z)=-1/[z-1/m_q(z)]. \tag{4}$$

This equation exhibits most clearly the fraction representation of correlators, which is the essence of the Zwanzig-Mori theory. It shows that there is a one-to-one correspondence between density fluctuations and force fluctuations. There is no separation between the time scales for the particle motion within cages and for the particles forming the cage. Therefore, the correlators $\phi_q(t)$ and the kernels $m_q(t)$ have to be calculated self-consistently—this is the essence of MCT. Equation (4) is scale invariant. With $\phi_q(t)$, $\phi_q^x(t)=\phi_q(x\cdot t)$ is also a solution for any $x>0$. The scale for the high-frequency dynamics is determined by the transient motion and this is governed by $M_q^{\mathrm{reg}}(t)$ and Ω_q or ν_q. But these quantities do not occur anywhere in Eq. (4). Thus, Eq. (4) can fix the solution only up to some time scale.

Equations (2) and (4) are the MCT equations for structural relaxation. In particular, they are the basis of the asymptotic expansions for the long-time dynamics for control parameters near bifurcation points.

B. The equations for structural relaxation near glass-transition singularities

In this section, the concept of a glass-transition singularity will be reviewed. The equations of motion will be rewritten in a form where the small quantities that characterize the relaxation near such a singularity appear transparently.

To simplify the notation of the following equations, the Laplace transform will be modified by a factor of $(-z)$:

$$\mathcal{S}[F(t)](z)=(-iz)\int_0^\infty \exp(izt)F(t)dt. \tag{5}$$

This linear mapping of functions of time to functions of frequency leaves constants invariant: $F(t)=c$ implies $\mathcal{S}[c](z)=c$. Let $F(t)=\langle X^*(t)X\rangle/(k_BT)$ denote a correlation function for variable X determined for temperature T. Then, the dynamical susceptibility for frequency ω can be written as $\chi(\omega)=F(t=0)-\mathcal{S}[F(t)](\omega+i0)$ [21]. Thus, $\mathcal{S}[F(t)](z)$ denotes the nontrivial part of a dynamical susceptibility.

Equation (4) can be rewritten as

$$\mathcal{S}[\phi_q(t)](z)/\{1-\mathcal{S}[\phi_q(t)](z)\}=\mathcal{S}[\mathcal{F}_q[V,\phi_k(t)]](z). \tag{6}$$

The equation $\phi_q(t\to\infty)=f_q$ is equivalent to $\mathcal{S}[\phi_q(t)](z\to 0)=f_q$. Similarly, one obtains $\mathcal{S}[\mathcal{F}_q[V,\phi_k(t)]](z\to 0)=\mathcal{F}_q[V,f_k]$. The $z\to 0$ limit of Eq. (6) yields a set of M implicit equations for the M glass form factors f_q [1]:

$$f_q/(1-f_q)=\mathcal{F}_q[V,f_k]. \tag{7}$$

This equation may have other solutions, say $\tilde{f}_q$. The glass form factor is distinguished by the maximum theorem: $\tilde{f}_q \leqslant f_q, q=1,\ldots,M$ [22].

Let V^c denote some reference state. The long-time limits of the correlators for this state shall be denoted by f_q^c. The correlators will be written in terms of new functions $\hat{\phi}_q(t)$:

$$\phi_q(t)=f_q^c+(1-f_q^c)\hat{\phi}_q(t). \tag{8}$$

The functional $\mathcal{F}_q[V,\phi_k(t)]$ can be rewritten as a Taylor series in $\hat{\phi}_k(t)$, using the coefficients

$$A^{(n)}_{qk_1\cdots k_n}(V)=\frac{1}{n!}(1-f_q^c)\{\partial^n\mathcal{F}_q[V,f_k^c]/\partial f^c_{k_1}\cdots\partial f^c_{k_n}\}\times(1-f^c_{k_1})\cdots(1-f^c_{k_n}). \tag{9a}$$

These will be split into the values for the reference state, $A^{(n)c}_{qk_1\cdots k_n}=A^{(n)}_{qk_1\cdots k_n}(V^c)$, and the remainders:

$$A^{(n)}_{qk_1\cdots k_n}(V)=A^{(n)c}_{qk_1\cdots k_n}+\hat{A}^{(n)}_{qk_1\cdots k_n}(V). \tag{9b}$$

Let us consider a path in control-parameter space given by $V(\epsilon)=(V_1(\epsilon),\ldots V_N(\epsilon))$. The N components of $V(\epsilon)$ are smooth functions of the path parameter ϵ, and the tangent vector $dV(\epsilon)/d\epsilon$ must not vanish. Let us choose $V(\epsilon=0)=V^c$, so that ϵ can be considered as a distance parameter specifying the neighborhood of V^c. One gets $V(\epsilon)=T\epsilon+\mathcal{O}(\epsilon^2)$, with $T=dV(0)/d\epsilon$ being the tangent vector of the path at V^c. The mode-coupling functional is a smooth function of V, i.e.,

$$\hat{A}^{(n)}_{qk_1\ldots k_n}(V)=\mathcal{O}(\epsilon). \tag{9c}$$

The details of the ϵ dependence of the coefficients are not important. The parameter ϵ is introduced mainly as a means for bookkeeping in the following expansions in $V-V^c$. Expanding the left hand side of Eq. (6) in powers of $\mathcal{S}[\hat{\phi}_q](z)$, one can rewrite this equation in the form

$$[\delta_{qk}-A^{(1)c}_{qk}]\mathcal{S}[\hat{\phi}_k(t)](z)=J_q(z), \tag{10a}$$

$$J_q(z)=\hat{A}^{(0)}_q(V)+\hat{A}^{(1)}_{qk}(V)\mathcal{S}[\hat{\phi}_k(t)](z)+\sum_{n=2}^{\infty}\{A^{(n)}_{qk_1\cdots k_n}(V)\mathcal{S}[\hat{\phi}_{k_1}(t)\cdots\hat{\phi}_{k_n}(t)](z)-\mathcal{S}[\hat{\phi}_q(t)]^n(z)\}. \tag{10b}$$

Here and in the following, summation over pairs of equal labels k is implied. These equations are equivalent to Eqs. (2) and (4) for the structural relaxation. The small quantities to be used for the asymptotic solution are the coefficients $\hat{A}^{(n)}_{qk_1\cdots k_n}$ and the functions $\hat{\phi}_q(t)$ or $\mathcal{S}[\hat{\phi}_q(t)](z)$, respectively.

Specializing Eqs. (10) to the $z\to 0$ limit, one gets the equation for $\hat{f}_q=\hat{\phi}_q(t\to\infty)$:

$$[\delta_{qk}-A_{qk}^{(1)c}]\hat{f}_k=\hat{A}_q^{(0)}(V)+\hat{A}_{qk}^{(1)}(V)\hat{f}_k + \sum_{n=2}^{\infty}[A_{qk_1\cdots k_n}^{(n)}(V)\hat{f}_{k_1}\cdots\hat{f}_{k_n}-\hat{f}_q^n]. \tag{11}$$

This is a rewriting of Eq. (7) so that small deviations of f_q from f_q^c and V from V^c are explicit. The $M\times M$ matrix $[\delta_{qk}-A_{qk}^{(1)c}]$ is the Jacobian of the set of implicit equations (7) for the reference solution f_q^c at $V=V^c$. This Jacobian consists of a unit matrix δ_{qk} and a matrix $A_{qk}^{(1)c}$ of positive elements. The Frobenius theorems imply that, generically, this matrix has a nondegenerate maximum eigenvalue $E^c>0$. All other eigenvalues have a modulus smaller than E^c [23]. It is a subtle property of MCT that $E^c\leqslant 1$ [24]. If $E^c<1$, the implicit-function theorem guarantees that all states V for sufficiently small ϵ are states whose long-time limits $f_q=f_q^c+(1-f_q^c)\hat{f}_q$ depend smoothly on ϵ. In the following, the reference state V^c will be specialized so that

$$E^c=1. \tag{12}$$

In this case, V^c is a bifurcation point of Eq. (7). The f_q are singular functions of ϵ for $\epsilon\to 0$, and therefore V^c is referred to as a glass-transition singularity. Since E^c is nondegenerate, the possible bifurcations are from the so-called cuspoid family $A_l, l=2,3,\ldots$. The bifurcation singularity A_l is topologically equivalent to that for the zeros of a real polynomial of degree l [2]. The A_2, also called the fold bifurcation, is the generic singularity obtained by varying a single control parameter. The liquid-glass transition of MCT is of this type. In this paper, the dynamics near a higher-order singularity $A_l, l\geqslant 3$, will be analyzed.

III. RELAXATION DESCRIBED BY ONE-COMPONENT MODELS

It will be shown in Sec. V that each iteration step of the asymptotic solution of the equations of motion splits into two parts. First, one has to reduce the problem of calculating M correlators to the one of calculating the projection of the correlators on the dangerous eigenvector of the above defined Jacobian. Second, one has to solve the equation for the projection. In this section, the second problem will be studied, which is equivalent to a discussion of $M=1$ models.

A. Classification of glass-transition singularities

One-component models deal with a single correlator $\phi(t)$, a single glass form factor f, etc. All matrix indices can be dropped in the formulas of Sec. II. The 1×1 matrix $A_{qk}^{(1)c}$ is identical with its maximum eigenvalue E^c. Because of Eq. (12), the left-hand side of Eq. (11) vanishes. The equation for $\hat{f}$ reads $\epsilon_1(V)+\epsilon_2(V)\hat{f}+\Sigma_{n\geqslant 2}[\hat{A}^{(n)}(V)-\mu_n]\hat{f}^n=0$, where the following abbreviations are used:

$$\mu_n=1-A^{(n)c},\quad \epsilon_n(V)=\hat{A}^{(n-1)}(V),\quad n=1,2,\ldots. \tag{13}$$

The singularity exhibited by $\hat{f}$ for ϵ tending to zero depends on the number of successive vanishing coefficients μ_n. A singularity of index $l, l\geqslant 2$, will be defined by

$$\mu_1=\mu_2=\cdots=\mu_{l-1}=0,\quad \mu_l\neq 0. \tag{14}$$

The equation for $\hat{f}$ reads

$$\mu_l\hat{f}^l=\epsilon_{l-1}(V)\hat{f}^{l-2}+\epsilon_{l-2}(V)\hat{f}^{l-3}+\cdots+\epsilon_1(V) + \left\{\epsilon_l(V)\hat{f}^{l-1}+\epsilon_{l+1}(V)\hat{f}^l+\sum_{n\geqslant l+1}[A^{(n)}(V)-1]\hat{f}^n\right\}. \tag{15}$$

The implicit-function theorem can be used to show that there is a smooth invertible transformation of the l variables $(\epsilon_1,\epsilon_2,\ldots,\epsilon_{l-1},\hat{f})$ which eliminates the curly brackets in Eq. (15). Thus, the singularities described by this equation are topologically equivalent to the ones described by the first line, i.e., by the zeros of a polynomial of degree l. In Arnol'd's terminology [2], such a singularity is referred to as A_l. Because of Eq. (9c), the $\epsilon_n(V)$ are of order ϵ and will be referred to as separation parameters.

The simplest glass-transition singularity is the A_2. In this case, there is only one relevant control parameter $\epsilon_1(V)$. One infers from Eq. (15) that there is a discontinuous change of $\hat{f}$ at the surface specified by $\epsilon_1(V)=0$. The bifurcation dynamics is characterized by power-law decay and there appear power-law dependencies of the relaxation scales on $|\epsilon_1(V)|$. All exponents in these laws are to be calculated from $\lambda=1-\mu_2$, which is called the exponent parameter [22]. The transition surface has a boundary that is determined by $\lambda=1$, i.e., by $\mu_2=0$. These end points are the higher-order singularities. The A_3 and A_4 are also referred to as cusp and swallow tail singularities, respectively.

B. Equations for an asymptotic solution

Let us specialize Eqs. (10a) and (10b) for $M=1$. Let us also express the coefficients $A^{(n)}(V)$ in terms of μ_n and $\epsilon_n(V)$:

$$\begin{aligned}0=&\epsilon_1(V)+(1-\mu_2)\mathcal{S}[\hat{\phi}^2(t)](z)-\mathcal{S}[\hat{\phi}(t)]^2(z)\\&+\epsilon_2(V)\mathcal{S}[\hat{\phi}(t)](z)+(1-\mu_3)\mathcal{S}[\hat{\phi}^3(t)](z)-\mathcal{S}[\hat{\phi}(t)]^3(z)\\&+\epsilon_3(V)\mathcal{S}[\hat{\phi}^2(t)](z)+(1-\mu_4)\mathcal{S}[\hat{\phi}^4(t)](z)-\mathcal{S}[\hat{\phi}(t)]^4(z)\\&+\cdots.\end{aligned} \tag{16}$$

This suggests an expansion of the solution in powers of $|\epsilon|^{1/2}$. With $G^{(n)}(t)=\mathcal{O}(|\epsilon|^{n/2})$, let us write

$$\hat{\phi}(t)=G^{(1)}(t)+G^{(2)}(t)+G^{(3)}(t)+\cdots. \tag{17}$$

The first line of Eq. (16) is of order $|\epsilon|$ and it provides a nonlinear integral equation for $G^{(1)}(t)$. The contributions to this line which are of order $|\epsilon|^{3/2}$ together with the leading terms of the second line provide a linear integral equation for $G^{(2)}(t)$, etc. This procedure will yield the desired asymptotic

expansion provided the indicated integral equations define meaningful solutions. This is indeed the case, as will be demonstrated below by explicit construction of the $G^{(n)}(t)$. To proceed, the following discussion will be restricted to higher-order singularities by requiring

$$\mu_2 = 0. \tag{18}$$

C. The leading contribution

The equation for the leading contribution to the correlator at a glass transition A_l with $l \geqslant 3$ reads

$$\epsilon_1(V) + \mathcal{S}[G^{(1)2}(t)](z) - \mathcal{S}[G^{(1)}(t)]^2(z) = 0. \tag{19}$$

The formulas for the Laplace transforms of the logarithm and its square imply $\mathcal{S}[\ln(t)](z) = \ln(i/z) - \gamma$ and $\mathcal{S}[\ln^2(t)](z) = \ln^2(i/z) - 2\gamma\ln(i/z) + \gamma^2 + (\pi^2/6)$, where $\gamma = 0.577\ldots$ is Euler's constant [cf. the Appendix, Eq. (A1)]. Hence, Eq. (19) is solved by $-B\ln(t)$ if $\epsilon_1(V) + (B^2\pi^2/6) = 0$. Since the correlators are monotonically decreasing functions of t [24], one must require $B > 0$. One concludes that a solution is given by

$$G^{(1)}(t) = -B\ln(t), \quad B = \sqrt{[-6\epsilon_1(V)/\pi^2]}, \tag{20}$$

provided the control parameters V obey

$$\epsilon_1(V) < 0. \tag{21}$$

A more general solution is $\tilde{G}^{(1)}(t) = G^{(1)}(t) + c$, where c can be any real constant. Introducing $x = \exp(-c/B)$, one gets $\tilde{G}^{(1)}(t) = G^{(1)}(xt)$. Thus, the generalization is the one implied by the scale invariance of the basic Eq. (4). It will not be considered here. Rather, it will be accounted for at the end of all calculations by rescaling t to t/τ. Ignoring corrections of order $|\epsilon|$, one derives from Eqs. (8), (17), and (20) the leading approximation for the correlator [6]:

$$\phi(t) = f^c - (1 - f^c)B\ln(t/\tau). \tag{22}$$

Let us anticipate that the smooth function $\epsilon_1(V)$ is generic for V near V^c and has a nonvanishing gradient. Then, $\epsilon_1(V) = 0$ defines a smooth surface through V^c in the control-parameter space. It separates the neighborhood of the glass-transition singularity V^c into a strong-coupling side where $\epsilon_1(V) > 0$ and a weak-coupling side where $\epsilon_1(V) < 0$. The results of this paper refer to the latter regime.

D. The leading correction

In order to solve Eq. (16) up to order $|\epsilon|^{3/2}$, one has to incorporate from the first line the contribution $2\mathcal{S}[G^{(1)}(t)G^{(2)}(t)](z) - 2\mathcal{S}[G^{(1)}](z)\mathcal{S}[G^{(2)}(t)](z)$, one has to evaluate the second line with $\hat{\phi}$ replaced by $G^{(1)}(t)$, and one can ignore all other terms. Hence, the equation for the leading correction $G^{(2)}(t)$ can be written in the form

$$\mathcal{T}[G^{(2)}(t)](z) = f^{(2)}(z). \tag{23}$$

Here, the linear integral operator $\mathcal{T}$ is defined by

$$\mathcal{T}[G(t)](z) = \mathcal{S}[\ln(t)G(t)](z) - \mathcal{S}[\ln(t)](z)\mathcal{S}[G(t)](z), \tag{24}$$

and the inhomogeneity of Eq. (23) reads

$$f^{(2)}(z) = -\Big\{ \epsilon_2(V)\mathcal{S}[G^{(1)}(t)](z) - \mu_3\mathcal{S}[G^{(1)3}(t)](z) + 2\zeta\{\mathcal{S}[G^{(1)3}(t)](z) - \mathcal{S}[G^{(1)}(t)]^3(z)\}\Big\}/(2B). \tag{25}$$

A factor of 2ζ has been introduced for later convenience. For the study of $M = 1$ models, one has to substitute $\zeta = 1/2$.

The solution of Eq. (19) was built on the equations $\mathcal{T}[c](z) = 0, \mathcal{T}[\ln t](z) = \pi^2/6$. These formulas are generalized in the Appendix by constructing polynomials $p_n(x)$ of degree $n \geqslant 1$ with the properties

$$p_n(x) = b_{n,1}x + b_{n,2}x^2 + \cdots + b_{n,n-1}x^{n-1} + x^n, \tag{26a}$$

$$\mathcal{T}[p_n(\ln(t))](z) = n(\pi^2/6)\ln^{n-1}(i/z). \tag{26b}$$

These polynomials are a convenient tool to solve the equation

$$\mathcal{T}[g(t)](z) = f(z) \tag{27a}$$

for inhomogeneities $f(z)$, which are polynomials in $\ln(i/z)$,

$$f(z) = \sum_{n=0}^{m} a_n \ln^n(i/z). \tag{27b}$$

Obviously,

$$g(t) = \sum_{n=1}^{m+1} [a_{n-1}/(n\pi^2/6)]p_n(\ln(t)). \tag{27c}$$

Using Eq. (20) and applying Eqs. (A1) and (A2) for the evaluation of the transformations of the powers of $\ln(t)$, one can write $f^{(2)}(z)$ in the form of Eq. (27b) for $m = 3$. The coefficients are linear functions of $\epsilon_1(V)$ and $\epsilon_2(V)$:

$$a_0 = [(6\zeta/\pi^2)(\Gamma_3 - \Gamma_1^3) - (3\mu_3/\pi^2)\Gamma_3]\epsilon_1(V) - (\Gamma_1/2)\epsilon_2(V), \tag{28a}$$

$$a_1 = [3\zeta - (9\mu_3/\pi^2)\Gamma_2]\epsilon_1(V) - (1/2)\epsilon_2(V), \tag{28b}$$

$$a_2 = -(9\mu_3/\pi^2)\Gamma_1\epsilon_1(V), \quad a_3 = -(3\mu_3/\pi^2)\epsilon_1(V). \tag{28c}$$

Here, $\Gamma_k = d^k\Gamma(1)/dx^k$ denotes the kth derivative of the gamma function at unity. One concludes that $G^{(2)}(t) = g(t)$, where Eq. (27c) is to be used with $m = 3$:

$$G^{(2)}(t) = \sum_{j=1}^{4} B_j \ln^j(t). \tag{29a}$$

The coefficients are derived with Eqs. (A7a)–(A7c):

$$B_1=(0.444\,25\zeta-0.065\,381\mu_3)\epsilon_1(V) - 0.222\,13\epsilon_2(V), \quad (29b)$$

$$B_2=(0.911\,89\zeta+0.068\,713\mu_3)\epsilon_1(V) - 0.151\,98\epsilon_2(V), \quad (29c)$$

$$B_3=-0.135\,04\mu_3\epsilon_1(V),$$

$$B_4=-0.046\,197\mu_3\epsilon_1(V). \quad (29d)$$

Dropping corrections of order $|\epsilon|^{3/2}$, the solution up to next-to-leading order reads

$$\phi(t)-f^c=(1-f^c)[(-B+B_1)\ln(t/\tau)+B_2\ln^2(t/\tau) + B_3\ln^3(t/\tau)+B_4\ln^4(t/\tau)]. \quad (30)$$

A singularity A_l with $l\geqslant 4$ implies $\mu_3=0$. In this case, the formula simplifies because $B_3=B_4=0$.

The described procedure can be continued. To solve Eq. (16) up to order ϵ^2, one derives the analog to Eq. (23): $\mathcal{T}[G^{(3)}(t)](z)=f^{(3)}(z)$. The function $f^{(3)}(z)$ has the form of Eq. (27b) with $m=6$, where the coefficients a_j depend on the parameters $\epsilon_1(V),\epsilon_2(V),\epsilon_3(V),\mu_3$, and μ_4. As a result, one gets

$$G^{(3)}(t)=\sum_{j=1}^{7} C_j\ln^j(i/z), \quad (31)$$

where $C_j=\mathcal{O}(|\epsilon|^{3/2})$.

IV. RESULTS FOR A ONE-COMPONENT MODEL

The simplest example for a generic cusp bifurcation is provided by an $M=1$ model with the mode-coupling functional $\mathcal{F}[V,\tilde{f}]=v_1\tilde{f}+v_3\tilde{f}^3$. This model was derived originally within a microscopic theory of spin-glass transitions [25]. It will be used here in order to demonstrate several implications of our theory. Let us use the model with a Brownian microscopic dynamics so that Eqs. (1b) and (2) specialize to

$$\tau_1\partial_t\phi(t)+\phi(t)+\int_0^t m(t-t')\partial_{t'}\phi(t')dt'=0, \quad (32a)$$

$$m(t)=v_1\phi(t)+v_3\phi^3(t). \quad (32b)$$

The two coupling constants $v_1\geqslant 0$ and $v_3\geqslant 0$ are considered as the components of the control-parameter vector $V=(v_1,v_3)$.

Figure 1 reproduces the phase diagram [6,22]. It is obtained from the largest of the solutions for f^c of Eq. (7), i.e., $v_1^c f^c+v_3^c f^{c3}=f^c/(1-f^c)$, and Eq. (12), i.e., $v_1^c+3v_3^c f^{c2}=1/(1-f^c)^2$, $0\leqslant f^c\leqslant 1$. There are two transition lines. The first one is the straight horizontal line of degenerate A_2 bifurcations: $v_1^c=1, 0\leqslant v_3^c\leqslant 4, f^c=0$. On crossing this line by increasing v_1, $f=\phi(t\to\infty)$ increases continuously. The second one is the smooth curve of A_2 singularities $V^{(2)c}$ shown as a heavy full line. It starts at $v_1^{(2)c}=0, v_3^{(2)c}=27/4, f^{(2)c}=2/3$. With decreasing $v_3^{(2)c}$, $f^{(2)c}$ decreases along the line. For $v_1^{(2)c}=1, v_3^{(2)c}=4$ one gets $f^{(2)c}=1/2$. Decreasing $f^{(2)c}$ further, the line reaches the end point that is marked by a circle. This is the A_3 singularity V^c specified by

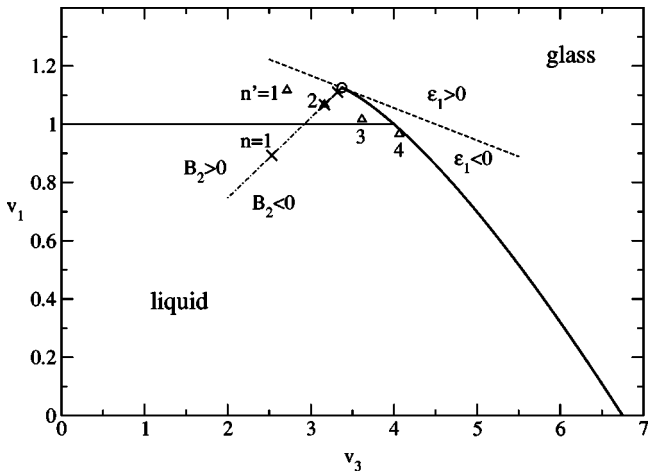

FIG. 1. Phase diagram for the one-component model defined in Sec. IV. The horizontal light full line marks the liquid-glass transition curve connected by a continuous variation of the glass form factor. The heavy full line presents the set of A_2 singularities, which ends at the A_3 singularity marked by a circle. The dashed straight line describes the points of vanishing separation parameter ϵ_1 and the dash-dotted one the points of vanishing coefficients B_2. Crosses with labels n and triangles with labels n' denote states discussed in Figs. 2–4 and Figs. 5 and 6, respectively.

$$v_1^c=9/8, \quad v_3^c=27/8, \quad f^c=1/3, \quad \mu_3=1/3. \quad (33)$$

The two separation parameters are obtained from Eqs. (9b) and (13) as linear functions of the parameters differences $\hat{v}_{1,3}=v_{1,3}-v_{1,3}^c$:

$$\epsilon_1(V)=(2/81)[9\hat{v}_1+\hat{v}_3], \quad \epsilon_2(V)=(4/27)[3\hat{v}_1+\hat{v}_3]. \quad (34)$$

These formulas determine the coefficient B in Eq. (20) and B_1-B_4 in Eqs. (29). The scales τ for the results in Eqs. (22), (30), and (31) are determined as the time where the correlator crosses the critical form factor: $\phi(\tau)=f^c$.

The dominant deviation of the correlators from the logarithmic decay law, Eq. (22), is caused by the term $B_2\ln^2(t/\tau)$ in Eq. (30). Thus, the logarithmic decay law is exhibited best for states V with $B_2=0$. This line is shown dash-dotted in Fig. 1. Figure 2 demonstrates the evolution of the dynamics upon shifting states on this line toward the A_3 singularity. The $\ln(t/\tau)$ interval, where Eq. (22) or (30) describes the correlators within an error margin of 5%, is marked by closed or open symbols, respectively. For $n\geqslant 2$, these intervals increase with decreasing $V-V^c$.

There are two peculiarities concerning the range of applicability of the asymptotic expansions. First, it can happen that for sufficiently large ϵ the range shrinks if one proceeds from the leading approximation to the next-to-leading one as

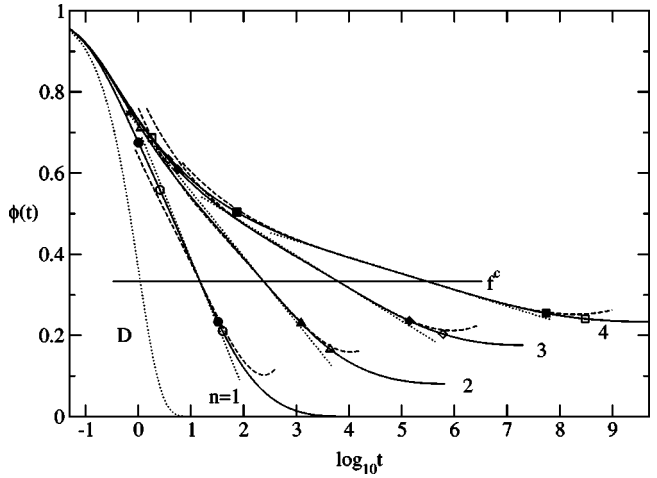

FIG. 2. Correlators $\phi(t)$ for the one-component model defined in Sec. IV. The states are located on the line $B_2=0$ with coupling constants $v_1^c-v_1=0.9298/4^n$, $v_3^c-v_3=3.3750/4^n$, $n=1,\ldots,4$, marked by crosses in Fig. 1. The full lines are the solutions of Eqs. (32a) and (32b) with $\tau_1=1$ as the unit of time, as also in the following figures. The dotted straight lines exhibit the leading approximation, Eq. (22), the dashed lines the leading correction, Eq. (30). The filled and open symbols, respectively, mark the times where these approximations deviate from the solution by 5%. The dotted line marked by D is the Debye law $\exp[-t/\tau_1]$. The horizontal line shows the critical form factor $f^c=1/3$.

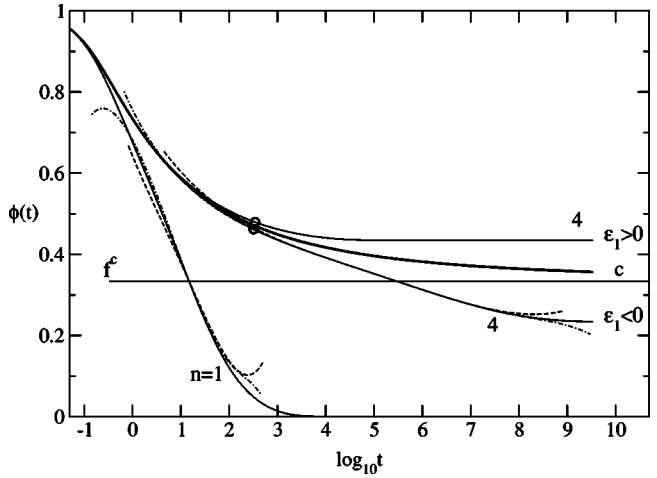

FIG. 3. The heavy full curve with label c is the solution of Eqs. (32a) and (32b) at the A_3 singularity, $V=V^c$, called the critical correlator. The thin full curves with labels $n=1$ and 4, $\epsilon_1<0$ reproduce two of the solutions discussed in Fig. 2. The dashed lines reproduce from Fig. 2 the corresponding approximations at next-to-leading order, Eq. (30). The dash-dotted curves extend the asymptotic expansion by including the second-order corrections, Eq. (31). The horizontal line marks the critical form factor $f^c=1/3$. The full curve marked with $n=4$, $\epsilon_1>0$ refers to a state $v_1-v_1^c=0.9298/4^4$, $v_3-v_3^c=3.3750/4^4$. The circles mark the times where the correlators $n=4$, $\epsilon_1\gtrless 0$ deviate by 2% from the critical one.

is demonstrated in Fig. 2 for the $n=1,2$ results. This is caused by a cancellation of errors due to neglecting the B_1 correction in the prefactor of the $\ln(t/\tau)$ term in Eq. (30) and due to neglecting the terms proportional to B_3 and B_4. This peculiarity would disappear if the tolerated error margin were decreased sufficiently below the 5% used. Second, for small $V-V^c$, the interval of decay for $\phi(t)$ below the critical form factor f^c that is described by the asymptotic expansion shrinks with decreasing separation. This is inferred by comparing the $n=3$ with the $n=4$ results. The reason is the following. The correlator $\phi(t)$ decreases monotonically toward its long-time limit f [24]. But the interval $f^c-f=-\hat{f}$ shrinks for $\epsilon\to 0$, since Eq. (15) implies $-\hat{f}=[-\epsilon_1(V)/\mu_3]^{1/3}[1+\mathcal{O}(\epsilon^{1/3})]$.

Figure 2 demonstrates that the transient regime extends to about $t/\tau_1=1$. For vanishing mode-coupling functional, the correlator describes a Debye process: $\phi(t)=\exp(-t/\tau_1)$. Mode-coupling effects cause a slower decay for $t/\tau_1\gtrsim 1$. But for V close to V^c, the transient dynamics is rather insensitive to changes of the coupling constants. There is a crossover interval, say $\tau_1<t<\tau^*$, before the decay of $\phi(t)$ toward f^c can be described by the $\ln(t/\tau)$ law. The beginning τ^* of the range of validity of Eq. (22) is indicated by the filled symbols. There are two subtleties demonstrated for $n\geqslant 2$. First, the time τ^* increases upon approaching the A_3 singularity, and therefore the decay interval $\phi(\tau^*)-f^c$ which is described by the logarithmic law shrinks with decreasing separation parameters. The control-parameter sensitive structural relaxation is governed by the two time scales τ^* and τ. Both times become large, but τ/τ^* becomes large as well for $\epsilon\to 0$. Second, the beginning of the range of applicability of the leading correction Eq. (30) is control-parameter insensitive, as is shown by the open symbols on the short-time part of the decay curves.

The explanation of the findings in the preceding paragraph is based on the fact that, for every fixed finite time interval, the MCT solutions are smooth functions of the control parameters [24]. Therefore, for ϵ tending to zero, the correlator for state V has to approach the correlator for state V^c, the so-called critical correlator. The latter is shown as the heavy full line with label c in Fig. 3. Thus, for every time interval $0\leqslant t\leqslant t_{\max}$ and every error margin, there exists an ϵ^* so that $\phi(t)$ agrees with the critical correlator within the error margin for all $|\epsilon|<\epsilon^*$ and all $0\leqslant t\leqslant t_{\max}$. This feature is demonstrated in Fig. 3 by the two curves with labels $n=4$ and $\epsilon_1\gtrless 0$. They refer to states with $v_1-v_1^c=\pm 0.9298/4^4$ and $v_3-v_3^c=\pm 3.3750/4^4$. These correlators are very close to the critical one for $t\leqslant t_{\max}$; $t_{\max}\approx 325$ is indicated by open circles in Fig. 3. The critical correlator does not exhibit a $\ln(t/\tau)$ part. Thus, the time τ^* for the onset of the description by Eq. (20) has to increase beyond any bound if ϵ tends to zero. The asymptotic expansion in Sec. III was based on $|\phi(t)-f^c|$ being small. This condition is satisfied for the critical correlator if the time is sufficiently large, since $\phi(V^c,t)$ decreases monotonically to f^c. Hence, for $\epsilon\to 0$ there must appear an increasing time interval $\tau_1<t<\tau^*$ where the asymptotic expansion describes the critical correlator. The ϵ dependence due to the separation parameters $\epsilon_n(V)$ and the ϵ dependence due to the time scale τ cancel to produce the critical correlator outside the transient regime and prior to the onset of the $\ln(t/\tau)$ law. This is shown

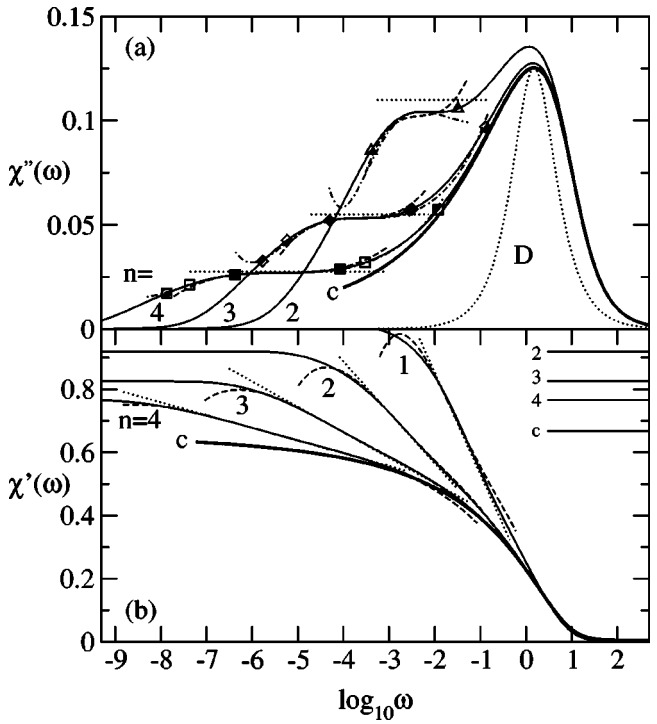

FIG. 4. Susceptibility spectra $\chi''(\omega)$ and reactive parts of the dynamical susceptibility $\chi'(\omega)$ for the one-component model defined in Sec. IV. The full lines with labels *n* and *c* correspond to the correlators with the same labels shown in Figs. 2 and 3. The dotted straight lines, the dashed lines, and the dash-dotted lines are the leading approximation Eq. (22), the leading correction Eq. (30), and the second correction Eq. (31), respectively. The filled, open, and half-filled symbols mark the frequencies where the corresponding approximation deviates from the spectrum by 5%. The dotted line with label *D* exhibits a Debye spectrum $C_D(\omega\tau_D)/[1+(\omega\tau_D)^2]$ with $C_D=0.2503$ and $\tau_D/\tau_1=0.670$ fitted to the maximum of the critical spectrum. The horizontal lines in the lower panel exhibit the static susceptibility $\chi'(\omega\to 0)=1-f$ for the states with labels $n=2$, 3, 4, and *c*, respectively.

most clearly by the dash-dotted lines in Fig. 3. They exhibit the result of the asymptotic expansion up to the second correction given by Eq. (31). They describe the complete decay for $t/\tau_1 \geqslant 1$ except for the final exponential approach toward $f=\phi(t\to\infty)$; and this is for states as far from the critical point as given by the one with label $n=1$ (cf. Fig. 1).

Figure 4 exhibits the dynamical susceptibilities $\chi(\omega)=1-\mathcal{S}[\phi(t)](\omega+i0)=\chi'(\omega)-i\chi''(\omega)$ for the states discussed above. Without interaction effects, the susceptibility spectrum shows a Debye peak $\chi''_D=C_D\omega\tau_D/[1+(\omega\tau_D)^2]$ with $C_D=1$, $\tau_D=\tau_1$. Such a Lorentzian spectrum is added to the upper panel as a dotted line with label *D*, where C_D and τ_D are fitted to the maximum of the critical susceptibility spectrum. This shows that the spectral peaks near $\omega=1$, in particular their high-frequency wings, are due to the transient dynamics. However, the low-frequency wings of the peaks are enhanced relative to the Debye spectrum and they are stretched to lower frequencies due to the critical relaxation within the interval $1/\tau^* < \omega < 1/\tau_1$. It is the structural relaxation near the A_3 singularity that causes the skewed shape of the spectral peaks. The leading approximation Eq. (22) implies constant-loss plateaus: $\chi''(\omega)/(1-f^c)=\pi B/2$. However, this formula describes the plateau only for $n\geqslant 3$ and then for a frequency interval that is considerably smaller than the time interval for which Eq. (22) describes the correlators in Fig. 2. The leading corrections in Eq. (30) are much more important for an adequate description of the spectra than for the approximation of the correlators. The second correction Eq. (31) is necessary to describe the plateau for the $n=2$ state within a 5% error margin. It is also necessary to describe the crossover of the spectrum from the plateau toward the critical one for $n=3,4$.

To understand the range of validity of Eq. (22) and its Fourier transform, one has to compare it with Eq. (30) and its Fourier transform, respectively. This amounts to comparing polynomials in $\ln(t/\tau)$ and $\ln(i/\omega\tau)$. Let us restrict ourselves to the dominant terms for the model to grasp the essence. Then one can write $(\phi(t)-f^c)/(1-f^c)=-B\ln(t/\tau)[1-(B_4/B)\ln^3(t/\tau)]$. Thus, within the error margin δ, the leading linear-in-$\ln(t/\tau)$ approximation holds for $|\ln(t/\tau)| \leqslant \sqrt[3]{\delta(B/B_4)}$. For the spectrum one gets from Eq. (A1) in leading order $\chi''(\omega)/(1-f^c)=B(\pi/2)[1-4(B_4/B)\ln^3(1/\omega\tau)]$. Hence, the spectrum is at the plateau within a deviation δ for $|\ln(1/\omega\tau)| \leqslant \sqrt[3]{\delta(B/4B_4)}$. As a result, the range of applicability on a logarithmic axis shrinks by a factor $\sqrt[3]{4}$ if one transforms from the time domain to the frequency domain.

Because of Eq. (A1), $\mathcal{S}[\ln^n(t/\tau)](z)=\ln^n(i/z\tau)-n\gamma\ln^{n-1}(i/z\tau)+\cdots$. In leading approximation for $t\to\infty$ and $z\to 0$, one finds $\chi'(\omega)\propto 1-\phi(1/\omega)$ whenever $\phi(t)$ is a polynomial in $\ln(t/\tau)$. This explains the lower panel of Fig. 4 as a different representation of Figs. 2 and 3. In particular, the linear-$\ln(\omega)$ parts in Fig. 4 are of a similar size to the linear-$\ln(t/\tau)$ parts in Fig. 2.

Let us consider the states labeled $n'=1$–3 and shown by triangles in Fig. 1 in order to analyze the implications of the correction term in Eq. (30) proportional to B_2. These states are chosen on the line $\epsilon_1=-0.0182$ and the state $n'=2$ is identical with state $n=2$ considered in Fig. 2 as an example for $B_2=0$. Figure 5 exhibits the correlators together with their approximations. For $B_2>0$, the $\phi(t)$ versus $\log(t)$ diagram is concave for all times outside the transient, since a parabola with positive curvature is added to the leading linear variation described by Eq. (22). The formula with the leading correction describes the complete structural relaxation, except for the very last piece for the approach to the long-time limit *f*, as shown by the curve $n'=1$. This observation also holds for cases with $B_2<0$ as is demonstrated for the state $n'=3$. However, for negative B_2, the $\phi(t)$ versus $\log_{10}(t)$ curve exhibits two inflection points because $\phi(t)$ crosses the critical form factor f^c with negative curvature. Since the $\phi(t)$ versus $\log(t)$ curve is convex for $\phi(t)\approx f^c$, it has to have an inflection point for $\phi(t)<f^c$ in order to approach the exponential, i.e., concave, long-time asymptote. It has to exhibit an inflection point also for $\phi(t)>f^c$ in order to approach the concave critical correlator for short times. The described alternation of convex and concave parts is identical to the behavior discussed earlier for the MCT correlators

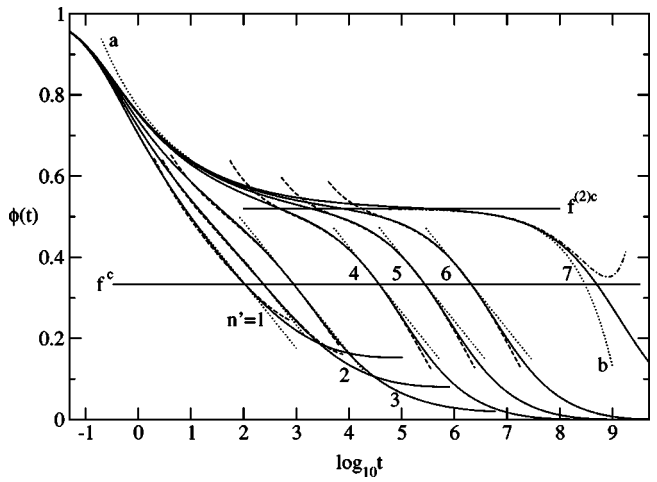

FIG. 5. Correlators $\phi(t)$ for the one-component model defined in Sec. IV for states located on the line $\epsilon_1=-0.0182$. The states with labels $n'=1-4$ have the coordinates $(v_1,v_3)=(1.1169, 2.7141),(1.0669, 3.1641),(1.0169, 3.6141)$, and $(0.9669,4.0641)$, respectively, and they are marked by triangles in Fig. 1. The state labeled $n'=2$ is identical with the state discussed in Figs. 1, 2, 4 with label $n=2$. The states with labels 5, 6, and 7 have the coordinates $(0.9599, 4.1271),(0.9569, 4.1541)$, and $(0.9549, 4.1721)$, respectively. The straight line through the states $1-7$ crosses the liquid-glass transition curve at the state $V^{(2)c}=(0.954\,66, 4.174\,07)$, where the critical glass form factor has the value $f^{(2)c}=0.520$. The exponent parameter for the A_2 glass-transition singularity is $\lambda=0.719$, implying a critical exponent $a=0.318$ and a von Schweidler exponent $b=0.608$. The critical decay law $\phi(t)-f^{(2)c}\propto t^{-a}$ and von Schweidler's law $\phi(t)-f^{(2)c}\propto -t^b$ are shown by dotted lines labeled *a* and *b*, respectively; the constants of proportionality are fitted to curve 7. The dash-dotted curve extends the von Schweidler expansion for curve 7 to $\phi(t)=f^{(2)c}-(t/\tilde{\tau})^b+1.48(t/\tilde{\tau})^{2b}$. The horizontal lines mark the critical glass form factors $f^{(2)c}$ and f^c, respectively. The dotted straight lines and the dashed curves are the leading asymptotic laws Eq. (22) and the leading correction Eq. (30), respectively.

for states near an A_2 bifurcation [22,26]. But, contrary to the characteristic decay pattern found for the MCT liquid-glass transition, the curve $n'=3$ does not show a two-step relaxation scenario, even though there is a huge stretching of the dynamics. For the decay from 0.80 to 0.05 a dynamical window of five orders of magnitude is required. Within this large window, the correlator follows closely the law $\phi(t)\propto\ln(t/\tau_{\rm eff})$.

The qualitative features described above for the state $n'=3$ are more pronounced for the state $n'=4$, since B_2 is decreased to larger negative values. The relaxation curve 4 has the form expected for states near a liquid-glass transition. To corroborate this statement, further states $5-7$ are considered on the line $\epsilon_1=-0.0182$ between the state 4 and the intersection $V^{(2)c}$ of this line with the liquid-glass transition curve. The transition point $V^{(2)c}$ is characterized by a critical glass form factor $f^{(2)c}>f^c$. The decay of the correlator from the value $f^{(2)c}$ to zero is the corresponding α process. Its initial part is described by von Schweidler's power law, as indicated in Fig. 5 for the curve $n'=7$ by the dotted line. In this case, von Schweidler's law accounts for the decay from $f^{(2)c}$ to about 0.45, i.e., for about 15% of the α relaxation. The analytical description of the α process can be expanded by using the extension of von Schweidler's law, $\phi(t)-f^{(2)c}\propto-(t/\tilde{\tau})^b+\tilde{B}(t/\tilde{\tau})^{2b}$ [26], as shown by the dash-dotted line. Asymptotically, the α process obeys the superposition principle: $\phi(t)=\tilde{\phi}(t/\tau_\alpha)$, where $\tilde{\phi}$ is the control-parameter-independent shape function. The $\phi(t)$ versus $\log(t)$ curves for the α process can be superimposed by rescaling the time, i.e., by shifts parallel to the $\log(t)$ axis. The reader can check that the curves $n'=4-7$ have the same shape for $\phi(t)<f^{(2)c}$. Outside the transient for $\phi(t)>f^{(2)c}$, the correlator follows the critical decay law for the fold bifurcation $\phi(t)-f^{(2)c}\propto 1/t^a$, as is also demonstrated for curve 7. The results for states $4-7$ exemplify the well understood scenario for the evolution of structural relaxation near a liquid-glass transition. The formula (30) provides an accurate description of 60% of the α process.

Comparison of the results for states $n'=1-3$ with the second-correction formula based on Eq. (31) yields the same conclusions as discussed above in connection with Fig. 3. The second-correction formula does not alter seriously the fit quality for the long-time part of the curves $n'=4-6$ in Fig. 5. However, for $\phi(t)\approx f^{(2)c}$, the extended formula yields slightly worse results than Eq. (30). This is so because for $\phi(t)\gtrsim f^{(2)c}$ the dynamics is governed by the A_2 singularity $V^{(2)c}$, whose existence is ignored in the expansions near the higher-order singularity V^c. The number $f^{(2)c}-f^c$ marks the limit where the expansion in the small parameter $\phi(t)-f^c$ makes sense. The opposite conclusion holds for the description of the α process for $\phi(t)\approx f^c$. von Schweidler's law results from an expansion for states V near $V^{(2)c}$ in terms of the small parameter $f^{(2)c}-\phi(t)$. This number becomes too large if $\phi(t)\approx f^c$. It is the dynamics dominated by the higher-order glass-transition singularity V^c that ruins the relevance of the expansion resulting in the von Schweidler law. The stretching of the α process connected with the transition of $V^{(2)c}$ is larger than estimated by von Schweidler's law, because of the logarithmic decay effects.

Figure 6 exhibits the susceptibility spectra calculated from the correlators discussed in Fig. 5. The results for the states $n'=1,2$, and 3 exhibit the evolution of an α peak if the states cross the line $B_2=0$ in the phase diagram of Fig. 1. The leading-correction formula Eq. (30) describes this scenario qualitatively. The spectra for states $n'=4,5$, and 6 exhibit the superposition principle for the α peak of the susceptibility spectra. The A_3 dynamics causes a high-frequency wing of the α peak closely following a linear variation with the logarithm of the frequency: $\chi''(\omega)\propto-\ln(\omega\tau)$. This phenomenon is described well by Eq. (30) and it causes a strong α-process stretching. The α-peak width at half of the α-peak height is about 2.5 decades. von Schweidler's asymptotic law is irrelevant for the description of the α peak for states $n'=4-6$.

V. RELAXATION FORMULAS FOR STATES NEAR HIGHER-ORDER GLASS-TRANSITION SINGULARITIES

In this section, the generalizations of Eqs. (22) and (30) will be derived for the asymptotic expansion of the solutions

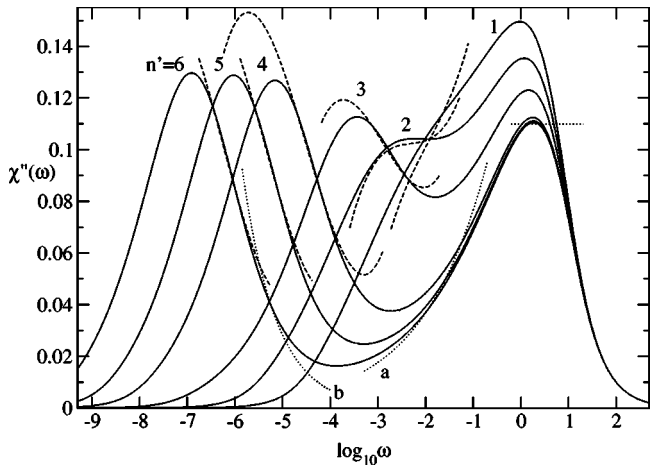

FIG. 6. Susceptibility spectra $\chi''(\omega)$ for the correlators in Fig. 5 for the labels $n'=1-6$. The dashed lines are obtained from the leading-correction formula Eq. (30). The dotted line with label *a* is the critical spectrum proportional to ω^a and the dotted line with label *b* is the von Schweidler law $\chi''(\omega)\propto\omega^{-b}$ for the state $n'=6$. The dotted horizontal line corresponds to the spectrum of the leading approximation Eqs. (20), (22), $\chi''(\omega)=(1-f^c)\sqrt{-6\epsilon_1}$, which is shared by all states $n'=1-6$.

dealing with an arbitrary number M of correlators. In particular, the general formulas for μ_2, μ_3, and ζ and for the separation parameters $\epsilon_1(V)$ and $\epsilon_2(V)$ will be obtained. The starting formulas are Eqs. (10a) and (10b). The subtlety of the problem is the treatment of the singular $M\times M$ matrix $[\delta_{qk}-A^{(1)c}_{qk}]$.

A. Asymptotic expansion of the equations of motion

The left and right eigenvectors of the matrix $A^{(1)c}_{qk}$ for the maximum eigenvalue $E^c=1$ will be denoted by a^*_k and $a_k, k=1,\ldots,M$, respectively. According to the Frobenius theorems [23], one can require $a^*_k\geqslant 0$ and $a_k\geqslant 0$. It will be convenient to fix the eigenvectors uniquely by the conditions $\Sigma_q a^*_q a_q=1$ and $\Sigma_q a^*_q a^2_q=1$. The solubility condition of Eq. (10a) reads

$$\sum_q a^*_q J_q(z)=0, \tag{35a}$$

and its general solution can be written as

$$\hat\phi_q(t)=a_q\hat\phi(t)+\tilde\phi_q(t). \tag{35b}$$

The splitting of $\hat\phi_q(t)$ into two terms is unique if one imposes the condition $\Sigma_q a^*_q\hat\phi_q(t)=\hat\phi(t)$. The part $\tilde\phi_q(t)$ can be expressed by means of the reduced resolvent R_{qk} of $A^{(1)c}_{qk}$:

$$\mathcal{S}[\tilde\phi_q(t)](z)=R_{qk}J_k(z). \tag{35c}$$

It is an elementary task to evaluate from matrix $A^{(1)c}_{qk}$ the vectors a^*_k, a_k and the matrix R_{qk} [23].

Equations (10b) and (35) suggest an expansion of $\hat\phi(t)$ as Eq. (17) and

$$\tilde\phi_q(t)=G^{(2)}_q(t)+G^{(3)}_q(t)+\cdots,$$

$$G^{(n)}_q(t)=\mathcal{O}(|\epsilon|^{n/2}), \tag{36a}$$

$$J_q(t)=J^{(2)}_q(t)+J^{(3)}_q(t)+\cdots,$$

$$J^{(n)}_q(t)=\mathcal{O}(|\epsilon|^{n/2}). \tag{36b}$$

Here, for example,

$$J^{(2)}_q(z)=\hat A^{(0)}_q(V)+A^{(2)c}_{qk_1k_2}a_{k_1}a_{k_2}\mathcal{S}[G^{(1)2}(t)](z) - a^2_q\mathcal{S}[G^{(1)}(t)]^2(z), \tag{37a}$$

$$\begin{aligned}J^{(3)}_q(z)=&2\{A^{(2)c}_{qk_1k_2}a_{k_1}a_{k_2}\mathcal{S}[G^{(1)}(t)G^{(2)}(t)](z)\\ &-a^2_q\mathcal{S}[G^{(1)}(t)](z)\mathcal{S}[G^{(2)}(t)](z)\}\\ &+\hat A^{(1)}_{qk}(V)a_k\mathcal{S}[G^{(1)}(t)](z)\\ &+2\{A^{(2)c}_{qk_1k_2}a_{k_1}\mathcal{S}[G^{(1)}(t)G^{(2)}_{k_2}(t)](z)\\ &-a_q\mathcal{S}[G^{(1)}(t)](z)\mathcal{S}[G^{(2)}_q(t)](z)\}\\ &+A^{(3)c}_{qk_1k_2k_3}a_{k_1}a_{k_2}a_{k_3}\mathcal{S}[G^{(1)3}(t)](z)\\ &-a^3_q\mathcal{S}[G^{(1)}(t)]^3(z).\end{aligned} \tag{37b}$$

The justification of the preceding expansions will be given by demonstrating how the equations can be solved recursively.

B. The leading-order contribution

The leading-order contribution to the solubility condition is obtained by substituting Eq. (37a) into Eq. (35a). One arrives at $\epsilon_1(V)+\lambda\mathcal{S}[G^{(1)2}(t)](z)-\mathcal{S}[G^{(1)}(t)]^2(z)=0$. Here $\lambda=\Sigma_q a^*_q A^{(2)c}_{qk_1k_2}a_{k_1}a_{k_2}$ is the expression for the exponent parameter [22,26] and

$$\epsilon_1(V)=\sum_q a^*_q\hat A^{(0)}_q(V). \tag{38}$$

The $z=0$ limit leads to $\epsilon_1(V)+(\lambda-1)\hat f^{(1)2}=0$. Comparison with Eq. (15) yields the conclusion that

$$\mu_2=1-\sum_q a^*_q A^{(2)c}_{qk_1k_2}a_{k_1}a_{k_2}. \tag{39}$$

This parameter has to be zero according to Eq. (18) in order for V^c to be a higher-order singularity. For $\mu_2=0$, $\lambda=1$, and the equation found for $G^{(1)}(t)$ is identical with Eq. (19). Thus, $\epsilon_1(V)$ is the first separation parameter and Eqs. (20) and (21) remain valid.

Introducing the critical amplitude h_q by the same formula as in the theory for the A_2-singularity [22,26]

$$h_q=(1-f^c_q)a_q, \tag{40}$$

the leading approximation for the correlators is

$$\phi_q(t) = f_q^c + h_q[-B\ln(t/\tau)]. \tag{41}$$

Here, $B=\sqrt{-6\epsilon_1(V)}/\pi=\mathcal{O}(|\epsilon|^{1/2})$. Equation (41) describes the dynamics up to errors of order ϵ; it is the generalization of the logarithmic decay law [6] to arbitrary MCT models.

Equation (41) is the factorization theorem of MCT. In leading order, $\phi_q(t)-f_q^c$ factorizes into two terms. The factor h_q is time and control-parameter independent and it characterizes the specific correlator via its q dependence. The other factor is the function $G^{(1)}(t)=-B\ln(t/\tau)$. This factor is shared by all correlators. It describes the control-parameter dependence via B and τ and the complete time dependence via $\ln(t)$. Within the range of validity of Eq. (41), the rescaled correlators $\hat{\phi}_q(1)=[\phi_q(t)-f_q^c]/h_q$ are the same for all q. Let us emphasize that Eq. (41) is an exact limit result for the solutions of Eqs. (1) and (2):

$$\lim_{\epsilon\to 0}[\phi_q(\tilde{t}\,\tau)-f_q^c]/\sqrt{-\epsilon_1(V)} = -\sqrt{6/\pi^2}\,h_q\ln(\tilde{t}). \tag{42}$$

The interval of rescaled times $\tilde{t}=t/\tau$, where $[\phi_q(t)-f_q^c]/\sqrt{-\epsilon_1(V)}$ becomes close to the right-hand side (RHS) of Eq. (42), expands beyond any bound if V approaches V^c arbitrarily close. It will be shown below, how the leading corrections for $\phi_q(t)$ describe violations of the factorization theorem.

Substitution of Eq. (37a) into Eq. (35c) yields the leading-order contribution to $\tilde{\phi}_q(t)$, i.e., the function $G_q^{(2)}(t)$ in Eq. (36a). Equation (19) is used to express $\mathcal{S}[G^{(1)}(t)]^2(z)$ in terms of $\mathcal{S}[G^{(1)2}(t)](z)$ so that

$$G_q^{(2)}(t) = X_q G^{(1)2}(t) + \hat{Y}_q(V). \tag{43a}$$

The amplitude X_q is independent of ϵ,

$$X_q = R_{qk}[A^{(2)c}_{kk_1k_2}a_{k_1}a_{k_2} - a_k^2]. \tag{43b}$$

$\hat{Y}_q(V)=\mathcal{O}(\epsilon)$ and reads

$$\hat{Y}_q(V) = R_{qk}[\hat{A}_k^{(0)}(V) - \epsilon_1(V)a_k^2]. \tag{43c}$$

C. The leading correction

If one substitutes Eq. (43a) into Eq. (37b), one gets an expression for $J_q^{(3)}(z)$ in terms of the known $G^{(1)}(t)$ and the unknown $G^{(2)}(t)$. Therefore, the solubility condition Eq. (35a) evaluated up to order $\epsilon^{3/2}$ yields an equation for $G^{(2)}(t)$. The latter has the form of Eq. (23), where also the inhomogeneity is given by Eq. (25). This holds with the formula

$$\epsilon_2(V) = \sum_q a_q^*\hat{A}^{(1)}_{qk}(V)a_k + 2\epsilon_1(V)\sum_q a_q^* a_q X_q + 2\sum_q a_q^*[A^{(2)c}_{qk_1k_2}a_{k_1}\hat{Y}_{k_2}(V) - a_q\hat{Y}_q(V)] \tag{44}$$

for the second separation parameter, and the constants

$$\zeta = \sum_q a_q^*[a_q X_q + a_q^3/2], \tag{45}$$

$$\mu_3 = 2\zeta - \sum_q a_q^*[A^{(3)c}_{qk_1k_2k_3}a_{k_1}a_{k_2}a_{k_3} + 2A^{(2)c}_{qk_1k_2}a_{k_1}X_{k_2}]. \tag{46}$$

As a result, Eqs. (29) for the function $G^{(2)}(t)$ remain valid.

Combining the results for $G^{(1)}(t), G^{(2)}(t)$, and $G_q^{(2)}(t)$ with Eq. (36a), and this with Eq. (8), one obtains the main result of this paper. It describes the correlators up to errors of order $|\epsilon|^{3/2}$:

$$\phi_q(t) = (f_q^c + \hat{f}_q) + h_q[(-B+B_1)\ln(t/\tau) + (B_2+K_qB^2)\times\ln^2(t/\tau) + B_3\ln^3(t/\tau) + B_4\ln^4(t/\tau)]. \tag{47}$$

Here

$$\hat{f}_q = (1-f_q^c)\hat{Y}_q \tag{48}$$

is a renormalization of the glass form factor of order ϵ to be calculated from Eq. (43c). The critical amplitude h_q is defined by Eq. (40). The parameter B_1 from Eq. (29b) is a renormalization of order ϵ of the prefactor of the logarithmic decay law. The three terms proportional to B_2, B_3, and B_4, respectively, describe leading deviations from the logarithmic decay. They are of order ϵ and follow from Eqs. (29c) and (29d). The relative size of these deviations is the same for all correlators. This means that these terms imply a modification of the factorization theorem $\phi_q(t)-(f_q^c+\hat{f}_q) = h_q G(t)$, in the sense that $G(t)=-B\ln(t/\tau)$ in Eq. (41) is to be generalized by the factor in square brackets on the RHS of Eq. (30). It is solely the contribution proportional to $B^2 = -6\epsilon_1/\pi^2=\mathcal{O}(\epsilon)$ that describes a violation of the factorization theorem. It enters with the correction amplitude

$$K_q = X_q/a_q. \tag{49}$$

Its q dependence expresses the fact that the size of the leading corrections depends on the chosen correlator. Thus, the range of validity of the universal Eq. (41) is not universal. The correction amplitude is to be calculated from Eq. (43b). The formula for K_q is the same as discussed in the theory for the A_2 singularity [26].

VI. RESULTS FOR A TWO-COMPONENT MODEL

The simplest example exhibiting a generic swallowtail bifurcation is given by an $M=2$ model with the mode-coupling functionals $\mathcal{F}_1[V,\tilde{f}_k]=v_1\tilde{f}_1^2+v_2\tilde{f}_2^2, \mathcal{F}_2[V,\tilde{f}_k] = v_3\tilde{f}_1\tilde{f}_2$. This model was motivated originally as a truncation of the microscopic equations of motion for a symmetric molten salt [27]. The model will be used here in order to demonstrate implications of our theory that could not be demonstrated for the $M=1$ model studied in Sec. IV. Using Brownian microscopic dynamics, the equations of motion (1b) and (2) read for $\phi_q(t), q=1,2$:

$$\tau_q \partial_t \phi_q(t) + \phi_q(t) + \int_0^t m_q(t-t')\partial_{t'}\phi_q(t')dt' = 0, \tag{50a}$$

$$m_1(t) = v_1\phi_1^2(t) + v_2\phi_2^2(t), \tag{50b}$$

$$m_2(t) = v_3\phi_1(t)\phi_2(t). \tag{50c}$$

The three coupling constants $v_n \geqslant 0$ will be considered as the components of the control-parameter vector $V=(v_1,v_2,v_3)$.

Let us note convenient equations for the discussion of the phase diagram [6,22], restricting ourselves to $v_3>4$. Equation (7) for the second form factor implies $f_2=[v_3f_1-1]/(v_3f_1)$, and this result can be used to eliminate f_2 in the following expressions. Thus, Eq. (7) for the first form factor $f_1/(1-f_1)=v_1f_1^2+v_2f_2^2$ is a linear equation for (v_1,v_2) with coefficients that are nonlinear in f_1 and v_3. The same statement holds for Eq. (12) for a singularity that is equivalent to $f_1^{(2)c}/(1-f_1^{(2)c})^2 = 2v_1^{(2)c}f_1^{(2)c2} + 2v_2^{(2)c2}f_2^{(2)c}(1-f_2^{(2)c})$. These equations can be used to express $v_1^{(2)c}$ and $v_2^{(2)c}$ in terms of $v_3^{(2)c}$ and $f_1^{(2)c}$. To ease the notation, variables x and y will be introduced as

$$v_3^{(2)c} = x, \quad f_1^{(2)c} = y. \tag{51a}$$

One gets

$$v_1^{(2)c} = \frac{3-(2+x)y}{2(1-y)^2y(2-xy)}, \tag{51b}$$

$$v_2^{(2)c} = \frac{x^2y(y^2-2y^3)}{2(1-y)^2(x^2y^2-3xy+2)}. \tag{51c}$$

These equations define the surface of bifurcation singularities of Eq. (7) in the three-dimensional parameter space. The variables x and y with $4<x$ and $1/2 \leqslant y \leqslant 3/(2+x)$ serve as surface parameters. The exponent parameter $\lambda = 1-\mu_2$ is determined by

$$\mu_2 = \frac{(3x^2+6x)y^3-(x^2+18x+8)y^2+(6x+18)y-6}{(2x^2+4x)y^3-12xy^2+(2x+4)y}. \tag{51d}$$

The maximum theorem, mentioned above in connection with Eq. (7), has to be used to identify among the points $(v_1^{(2)c},v_2^{(2)c},v_3^{(2)c})$ those that are glass-transition singularities.

Figure 7 exhibits three cuts through the parameter space. The cut $v_3=20$ is typical for sufficiently small values of x. The cut through the bifurcation surface yields a smooth curve of A_2 glass-transition singularities. The bifurcation surface for such $v_3^{(2)c}$ deals solely with the generic scenario for liquid-glass transitions.

The cut shown for $v_3=45$ is representative for sufficiently large values of x. In this case, the cubic numerator polynomial in Eq. (51d) has two zeros $y_1(x)<y_2(x)$ above some y_0; they can be evaluated elementarily [28]. The transition line consists of several pieces. The first one, obtained for

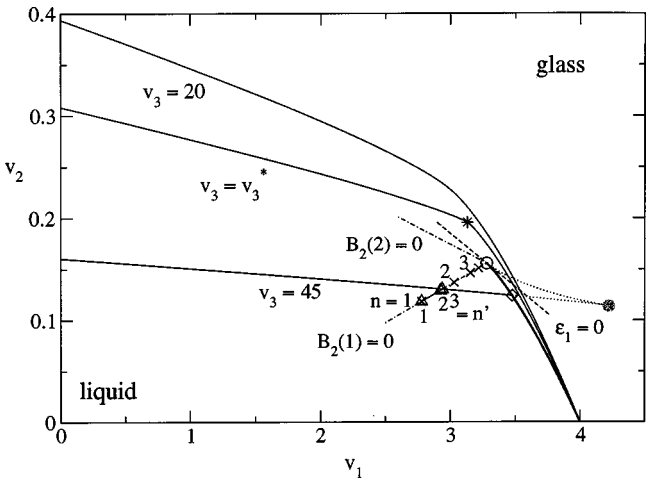

FIG. 7. Phase diagram for the two-component model defined in Sec. VI. The full lines are cuts through the bifurcation surface for $v_3=20$, $v_3=v_3^*$, and $v_3=45$, respectively. The value $v_3^*=24.7\ldots$ denotes a coordinate of the A_4 singularity indicated by a star. For $v_3>v_3^*$, there occur A_3 glass-transition singularities as indicated for $v_3=45$ by an open circle. The transition lines exhibit a crossing point shown as an open diamond. The dotted lines that join at the cusp singularity marked by a shaded circle complete the bifurcation diagram of Eq. (7), but they have no relevance for the discussion of the MCT solutions (see text). The dashed line denotes the $v_3=45$ cut through the surface of vanishing first separation parameter ϵ_1. The dash-dotted lines are the cuts $v_3=45$ through surfaces of the vanishing leading correction term $B_2(q)=B_2+K_qB^2$ in Eq. (47), $q=1,2$. The crosses labeled $n=1,2,\ldots$ and triangles labeled $n'=1,2,3$ mark states whose dynamics is discussed in Figs. 8 and 9,10, respectively.

$1/2 \geqslant y > y_2(x)$, is shown in Fig. 7 as a heavy full line. It starts at $v_1^{(2)c}=4$, $v_2^{(2)c}=0$ and ends at the A_3 singularity marked by a circle. The second piece describes bifurcations with $\mu_2<0$ for $y_2(x)>y>y_1(x)$. It connects the mentioned A_3 singularity with a second A_3 singularity of Eq. (7) that is shown as a shaded circle. This piece of the line is shown dotted. Decreasing y further, one gets a curve with $\mu_2>0$ that joins the second A_3 singularity with the point $v_1^{(2)c}=0$, $v_2^{(2)c}=3/(2+x)$. This line exhibits a crossing point with the first line piece mentioned above, which is shown as a diamond. The part between the second A_3 singularity and the crossing point is shown dotted, and the final piece is shown as a light full line. The dotted bifurcation lines and the second A_3 singularity are excluded from the set of glass-transition singularities because of the maximum theorem. These items have been added to the figure merely in order to allow the reader to recognize the familiar swallowtail scenario [2]. The crossing point organizes three lines of fold singularities. Between the A_3 singularity and the crossing point, there is a line of glass-glass transitions. The continuation of the line to the boundary of the admissible parameter range $v_2=0$ deals with liquid-glass transitions. The third line between the crossing point and the parameter boundary at $v_1=0$ also deals with liquid-glass transitions. Both lines are characterized by a discontinuous increase of the correlators' long-time limits from zero to the positive critical glass form factors $f_q^{(2)c}>0$.

Decreasing x from large values to smaller ones, the two cusp values $y_1(x)$ and $y_2(x)$ approach each other. The corresponding parameter vectors $V^c=(v_1^c(x),v_2^c(x),v_3^c(x))$ form curves that approach each other with decreasing x and join at a certain value x^*: $y_1(x^*)=y_2(x^*)=y^*$. The pair (x^*,y^*) defines the A_4 singularity for the model. The parameters for this singularity are obtained if the derivative of the numerator polynomial in Eq. (51d) is zero for $\mu_2=0$. This leads to $(x^*-2)(x^*-4)(x^{*4}-30x^{*3}+136x^{*2}-168x^*+88)=0$. The elementary solution for the zeros of the quartic polynomial [28] determines the coordinates of the swallowtail singularity $x^*=24.779\,392\ldots, y^*=0.242\,663\,25\ldots$. The cut through the transition surface for $v_3=x^*$ is shown in Fig. 7 as a pair of light full lines joining at the A_4 singularity which is indicated by a star.

Figure 8 demonstrates the validity of the factorization theorem for states close enough to a cusp singularity V^c and its violation for states sufficiently away from it. For the A_3 singularity with $v_3^c=45$, the correction amplitudes calculated from Eq. (49) are quite different for the two correlators: $K_1=0.068\,57, K_2=-2.049$. Therefore, the lines for vanishing dominant correction, i.e., the cut of the surfaces $B_2(q)=B_2+K_qB^2=0, q=1,2$, with the plane $v_3=45$, are quite different as well, as shown by the dash-dotted lines in Fig. 7. The four states discussed in Fig. 8 are chosen on the surface $B_2(1)=0$. Thus, the scenario for the evolution of the $\ln(t/\tau)$ law shown for $\phi_1(t)$ is in qualitative agreement with the one discussed in Fig. 2. The states with labels $n=3$ and 4 are so close to the singularity, that the correction term in Eq. (47) proportional to $B_2(2)=\mathcal{O}(\epsilon)$ is not important. As a result, the rescaled functions $[\phi_q(t)-f_q^c]/h_q$, $q=1$ and 2, agree for the states $n=3$ and 4, and the same holds for the corresponding approximations. However, for the states with labels $n=1$ and 2, the negative coefficient $B_2(2)$ is so large that the $\phi_2(t)$ versus $\log_{10}(t)$ curve does not exhibit the straight line obtained for $\phi_1(t)$ versus $\log(t)$ diagram. Rather, the correlator $\phi_2(t)$ exhibits changes of curvature and inflection points as explained above in Fig. 5 for the state $n'=3$.

Figure 8 also exemplifies a problem concerning the choice of the time scale τ. The complete solution of Eqs. (2) and (4) is unique up to the choice of a control-parameter independent time scale. The nonlinear coupling of the correlators of different index q requires scale universality. However, if a time scale like τ is deduced from some approximation to the equation of motion, the error of the approximation will result in violations of the scale universality for the approximate solutions. In constructing the approximate solutions in Fig. 8—and also in the upper panel of Fig. 9—the time τ was fixed for the leading approximation from $\phi_1(\tau)=f_1^c$ and for the leading correction from $\phi_1(\tau)=f_1^c+\hat{f}_1$. The errors explained lead to offsets for the second correlator: $\phi_2(\tau)\neq f_2^c$ and $\phi_2(\tau)\neq f_2^c+\hat{f}_2$, respectively, for the two approximations studied. This explains, e.g., why the dashed line for $\phi_2(t)$ for the state $n=1$ does not coincide with the full one. One could also choose τ differently, e.g., by requesting $\phi_2(\tau)=f_2^c+\hat{f}_2$ as was done in the lower panel of Fig. 9.

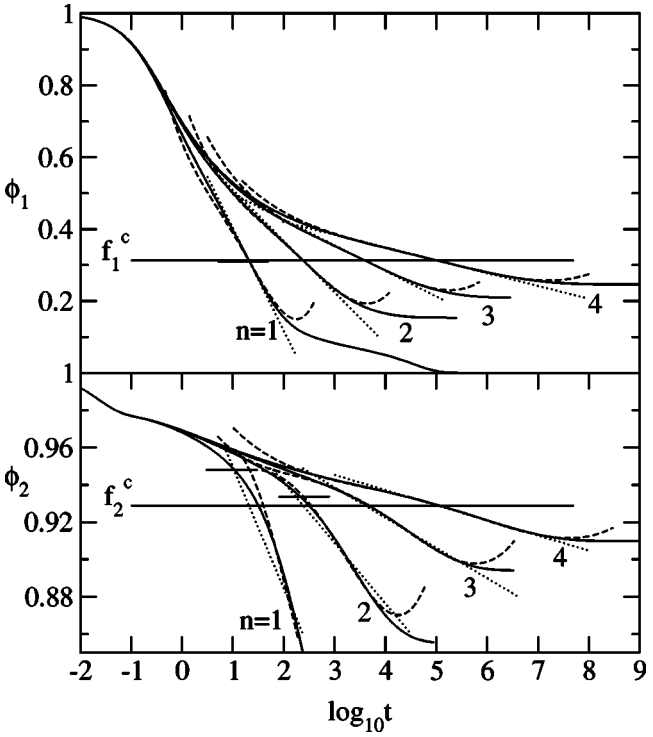

FIG. 8. Correlators $\phi_{1,2}(t)$ for the two-component model defined in Sec. VI. The states labeled $n=1,\ldots,4$ are located on the cut $v_3=45$ through the surface of vanishing dominant correction for the first correlator, $B_2(1)=B_2+K_1B^2=0$. The coupling constants are $v_1^c-v_1=2/4^n, v_2^c-v_2=0.149\,07/4^n$ and the states for $n=1,2$, and 3 are shown in Fig. 7 by crosses. The full lines are the solution of Eqs. (50a)–(50c). The dotted straight lines show the leading approximation Eq. (41) and the dashed ones the leading correction Eq. (47). The long horizontal lines show the critical glass form factors $f_1^c=0.312\,507$, $f_2^c=0.928\,89$ and the short horizontal lines shown for the states $n=1,2$ denote the renormalized form factors $f_{1,2}^c+\hat{f}_{1,2}$ according to Eq. (48). Here and in the following figures, the model is used with $\tau_1=\tau_2=1$.

The transition line which is shown in Fig. 7 by the light full and almost horizontal curve for the cut $v_3=45$ intersects the line $B_2(1)=0$ at some glass-transition singularity $V^{(2)c}=(2.94\ldots,0.130\ldots,45.0)$. For states on the line $B_2(1)=0$ that are close enough to this singularity, one gets the standard liquid-glass transition scenario, i.e., the evolution of a plateau of the $\phi_q(t)$ versus $\log(t)$ diagram at the critical glass form factor $f_q^{(2)c}$ and an α process for the decay below this plateau. The universal bifurcation results for an A_4 singularity require that the plateau values are below the critical form factors of the nearby A_3 singularity: $f_q^{(2)c}<f_q^c$. For the example under discussion, one gets $f_1^{(2)c}=0.0747$, $f_2^{(2)c}=0.7027$ and $f_1^c=0.3125$, $f_1^c=0.9289$. The precursor of the liquid-glass transition at $V^{(2)c}$ explains the stretched tail exhibited in Fig. 8 for the decay of $\phi_1(t)$ below 0.1 for the state $n=1$.

To corroborate the discussion of the preceding paragraph, the correlators with label $n=1$ are reproduced as curves with label $n'=1$ in Fig. 9. Two further curves with labels $n'=2$ and 3 are added. They refer to states between state 1 and the

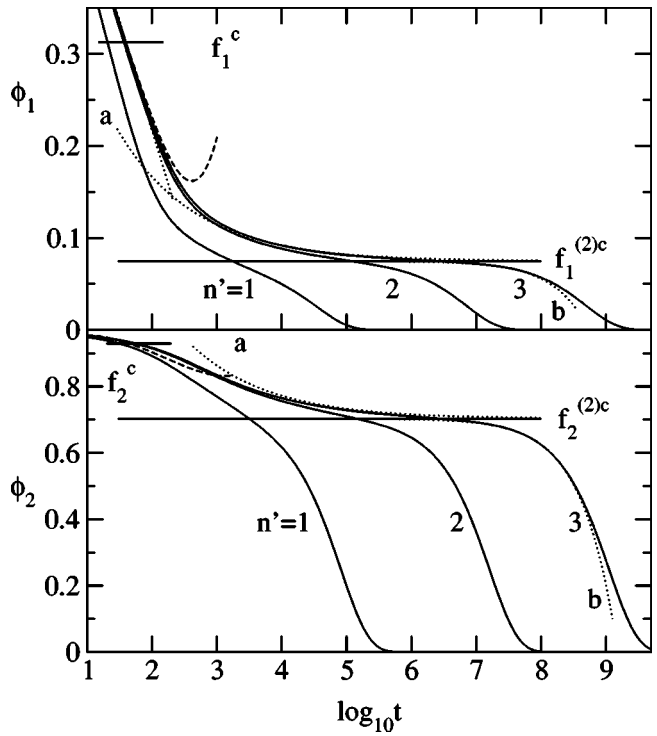

FIG. 9. Correlators for the two-component model defined in Sec. VI. The states with labels $n'=1,2$, and 3 are located on the line defined by $v_3=45, B_2(1)=0$ and have coordinates $(v_1,v_2)=(2.7799, 0.1183), (2.9254, 0.1292)$, and $(2.9391, 0.1302)$, respectively. They are indicated in Fig. 7 by triangles and approach the liquid-glass transition point $V^{(2)c}$ with coordinates $v_1^{(2)c}=2.941\,029$, $v_2^{(2)c}=0.130\,326$. The state $n'=1$ is identical to state $n=1$ discussed in Fig. 8. The horizontal lines show the critical glass form factors f_q^c and $f_q^{(2)c}$, $q=1,2$, for the cusp singularity V^c and the fold singularity $V^{(2)c}$, respectively. The liquid-glass transition point is connected with an exponent parameter $\lambda=0.603$, leading to the exponents $a=0.363$ and $b=0.807$. The critical decay laws $[\phi_q(t)-f_q^{(2)}c]=h_q^{(2)c}(t_0/t)^a$ are shown as dotted lines labeled *a*. The von Schweidler laws $[\phi_q(t)-f_q^{(2)}c]/h_q^{(2)c}\propto -t^b$ with a time scale fitted for the curve $n'=3$ are shown as dotted lines with the label *b*. The straight dotted line in the upper panel exhibits the leading asymptotic law Eq. (41) for $\phi_1(t)$ and the state $n'=3$; the dashed line shows the result of Eq. (47). The dashed lines in the lower panel exhibit the leading-correction formulas Eq. (47) for $\phi_2(t)$ and states $n'=1$ and 3, respectively.

transition point $V^{(2)c}$ as denoted in Fig. 7 by triangles. The diagrams for $\phi_1(t)$ for states 2 and 3 exhibit the two-step-relaxation scenario characteristic for an A_2 bifurcation. The decay for $\phi_q(t)<f_q^{(2)c}$ demonstrates the superposition principle for the α process, and its initial part can be described by von Schweidler's power law. The decay toward the plateaus $f_q^{(2)c}$ for $t>1000$ follows the critical law for the A_2 singularity $V^{(2)c}$. The universal laws for the dynamics near a fold bifurcation imply that the correlators follow the asymptote of the critical law $[\phi_q(t)-f_q^{(2)c}]/h_q=(t/t_0)^{-a}$ for short times down to about one decade above the end of the transient dynamics, i.e., until about $t=10$. In particular, for small times, the correlator for state $n'=2$ should approach the one for state $n'=3$. However, these features are not exhibited in Fig. 9. Rather, the t^{-a} law becomes irrelevant for the description of the dynamics below times around 10^3, where the A_2 critical curve crosses the curves describing the logarithmic laws for the A_3 singularity. As a result, there appears a window between the end of the transient and the beginning of the description by the A_2 singularity results where the correlators are described by Eq. (47). This window deals with an increase in time over about two orders of magnitude. In this window, the logarithmic decay processes destroy the manifestation of the t^{-a} law.

The lower panel of Fig. 9 demonstrates a further implication of V^c dynamics on the precursors of the liquid-glass transition dynamics. Even though the time scale for the α process for the states $n'=1$ or 2 exceeds the one for the transient by factors 10^4 and 10^6, respectively, the correlator $\phi_2(t)$ does not exhibit the two-step scenario for these states. Rather, there is a large time interval where the approach toward the plateau $f_2^{(2)c}$ follows closely the law $[\phi_2(t)-f_2^{(2)c}]\propto\ln(t/\tau_{\rm eff})$. This is due to cancellation of two effects: The asymptotes for the V^c dynamics and for the $V^{(2)c}$ dynamics yield a positive curvature, while the onset of the α process causes a negative one. The resulting nearly linear-log(t) variation must not be mistaken as the true asymptotic logarithmic law given by Eq. (41).

The destruction of the critical decay law of the liquid-glass transition dynamics by the presence of a higher-order glass-transition singularity nearby alters the familiar pattern of the susceptibility spectra, as shown in Fig. 10. The Debye peak for the transient dynamics deals with the spectra for $\omega>0.1$, as shown by the peak around $\omega\approx 1$ for $\chi_1''(\omega)$. This peak is strongly suppressed and shifted to higher frequencies for $\chi_2''(\omega)$. There is the large frequency regime $-4\leqslant\log_{10}\omega\leqslant -1$, where the ω^a law is irrelevant for the description of the structural relaxation spectrum. Rather, the critical relaxation spectrum of the cusp singularity leads to a high spectral enhancement of $\chi_1''(\omega)$ relative to the ω^a spectrum; it leads to a second structural relaxation peak near $\omega\approx 0.01$ in addition to the low-frequency α peak. It was discussed in connection with the states $n'=3$ and 4 in Figs. 5 and 6, that the winding of the $\phi(t)$ versus $\log(t)$ curve around an effective $\ln(t)$ law for states with $B_2<0$ is a precursor phenomenon of a nearby A_2 transition singularity. Indeed, the spectrum $\chi_2''(\omega)$ exhibits the α peak of the mentioned transition with a maximum for $\log_{10}\omega\approx -3$. Thus, because of $B_2(2)<0$, the susceptibility for the second correlator exhibits two α peaks, referring to the two parts of the liquid-glass transition lines discussed in Fig. 7. The low-frequency α peaks shift strongly with changes of $n'=1,2$, and 3, since the states are shifted toward the transition singularity $V^{(2)c}$ on one of the lines. The high-frequency α peak does not change significantly since the distance of the states from the other transition line is almost unaltered. As explained in connection with Fig. 6, the leading correction formula Eq. (47) describes the high-frequency wing of the second α peak.

VII. CONCLUSIONS

Describing the states of a system by a vector V of control parameters, the neighborhood of a glass transition singularity

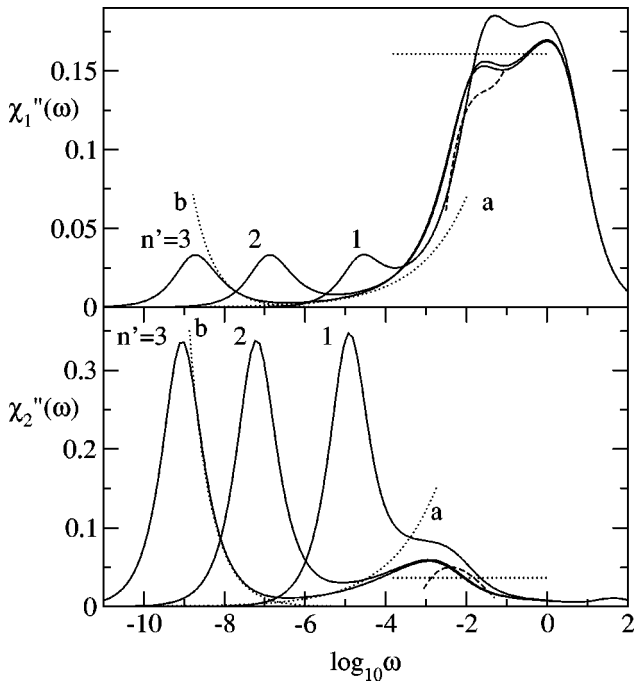

FIG. 10. Susceptibility spectra for the correlators shown in Fig. 9.

V^c was characterized by a sequence of separation parameters $\epsilon_1(V), \epsilon_2(V), \ldots$. These are smooth functions of V that vanish at V^c, and they are considered as small of order ϵ. The glass-transition singularities V^c are the bifurcation points of the glass form factors $f_q(V)=\phi_q(t\to\infty)$, i.e., of the long-time limits of the correlators $\phi_q(t)$. These bifurcations are of the cuspoid family $A_l, l=2,3\ldots$. The $\epsilon_1, \ldots, \epsilon_{l-1}$ are the relevant small coefficients specifying the polynomial of degree l whose largest zero determines $f_q(V)$ for small ϵ. The major result is the proof that the solution of the MCT equations can be asymptotically expanded in polynomials $P(x)$ of the logarithm of time, $x=\ln(t/\tau)$, for states close to an $A_l, l\geqslant 3$, and $\epsilon_1(V)<0$. The leading term of order $|\epsilon|^{1/2}$ yields the $\ln(t/\tau)$ law Eq. (41). The prefactor for this polynomial of degree 1 is given solely by the first separation parameter $\epsilon_1(V)$. The leading correction adds a polynomial of degree 4. The coefficients are of order $|\epsilon|$, and they are determined by $\epsilon_1(V)$ and $\epsilon_2(V)$, Eqs. (29) and (47). The second correction adds a polynomial of order 7; the coefficients are of order $|\epsilon|^{3/2}$ and determined by $\epsilon_1(V), \epsilon_2(V), \epsilon_3(V)$, and so on. Several relaxation scenarios have been identified that are utterly different from the MCT scenario for the liquid-glass transition. The latter is described by an A_2 singularity.

There are distinct surfaces in parameter space, where the prefactor of the x^2 monomial in the polynomial $P(x)$ vanishes. For this case, the $\ln(t/\tau)$ law dominates the dynamics for such times where $\phi_q(t)\approx f_q(V^c)$. This law may describe the complete decay except for the transient and for the final exponential approach of $\phi_q(t)$ toward its long-time limit, Fig. 2. States near the mentioned surface exhibit slight deformations of the straight $\phi(t)$ versus $\log_{10}(t)$ curve. There is a concave behavior on one side of the surface and a winding around the straight line with alternating convex and concave parts on the other side, as shown for the states $n'=1-3$ in Fig. 5. The corrections to the leading-order asymptotic results depend on the correlator under consideration. The surfaces of dominant $\ln(t/\tau)$ behavior are different for different correlation functions, as explained in connection with Fig. 8.

Every higher-order glass-transition singularity V^c is an end point of a surface of fold-bifurcation points $V^{(2)c}$ with $f_q(V^c)=f_q^c<f_q^{(2)c}=f_q(V^{(2)c})$. For states sufficiently close to $V^{(2)c}$, one finds the standard transition scenario with two-step relaxation described by the interplay of α- and β-scaling laws. The correlators for $\phi_q(t)\approx f_q^c$ are a part of the α process. Therefore, the logarithmic decay laws as formulated by Eq. (47) describe the α-relaxation master functions. They reduce the range of validity of von Schweidler's power law and cause anomalies of the α-relaxation shape functions as shown for the states $n'=4-6$ in Figs. 5 and 6.

Generically, near a higher-order singularity V^c, there is a further surface of fold bifurcations that crosses the transition surface discussed in the preceding paragraph, Fig. 7. As a result, there is the scenario for transition singularities of type A_2, but now with critical form factors smaller than the ones at V^c: $f_q^{(2)c}<f_q^c$. Consequently, the logarithmic decay laws are a part of the relaxation toward the plateau $f_q^{(2)c}$. They reduce the range of applicability of the critical decay and introduce a large crossover interval for structural relaxation between the end of the transient and the beginning of the transition dynamics caused by $V^{(2)c}$, as is demonstrated in Figs. 9 and 10 for the correlator $\phi_1(t)$. In particular, there can be a crossover from the transient to a simple $\ln(t/\tau)$ law followed by a crossover to a von Schweidler power law. This scenario was demonstrated by the experiments reported in Ref. [16] and by numerical solutions of MCT equations for the square-well liquid in Ref. [19]. There can also be a susceptibility spectrum for structural relaxation consisting of two peaks, as shown for $\chi_2''(\omega)$ in Fig. 10.

The asymptotic expansion also describes the critical correlator of the higher-order glass-transition singularity outside the transient, Fig. 3. These correlators deal with the decay toward f_q^c for control parameters at the singularity. For states with $\epsilon_1>0$, $\phi_q(t)$ follows the critical decay until close to its intersection with the long-time asymptote $\phi_q(t\to\infty)=f_q>f_q^c$. Here it crosses over rapidly to the glass form factor f_q. Summarizing, the formulas of this paper provide a qualitative understanding of the decay of the correlations provided the state V of the system is close to a higher-order glass-transition singularity and the correlator $\phi_q(t)$ is close to the glass form factor f_q^c at this singularity.

Let L_t denote the length of the $\log(t)$ interval where an approximation by one of the polynomials $P(\ln(t/\tau))$ describes the solution for the correlator $\phi_q(t)$. Let L_ω denote the length of the $\log(\omega)$ interval where the Fourier cosine transform of $P(\ln(t/\tau))$ leads to a description of comparable accuracy for the susceptibility spectrum $\chi_q''(\omega)$. It was explained in connection with Fig. 4 that L_ω is considerably smaller than L_t. This phenomenon for glassy dynamics was discussed earlier for the liquid-glass transition [26], but it is

more pronounced for the higher-order singularities. This feature of stretched relaxation is the reason why it is more difficult to test asymptotic MCT formulas with data for spectra than it is with data for correlators in the time domain.

If there is a higher-order glass-transition singularity in a disordered system, there is no generic path for the evolution of the structural relaxation. Only a parameter surface can be generic for the description of the dynamics near a cusp singularity. One has to vary two independent parameters to identify an A_3 singularity, three parameters to identify an A_4 bifurcation, and so on. We hope that the demonstration of all basic scenarios for the dynamics near an A_3 singularity will be of use to identify such singularities in colloids, if there are any. In this case, the derived formulas are elementary enough for data fitting. Such fitting might lead to a judgment on the relevance of the subtle implications of mode-coupling theory for the discussion of glass-forming systems.

ACKNOWLEDGMENTS

We thank C. Hagedorn for assistance and S.-H. Chong, M. Fuchs, A. M. Puertas, and Th. Voigtmann for helpful discussions. Our work was supported by the Deutsche Forschungsgemeinschaft Grant No. Go154/13-1.

APPENDIX: LAPLACE TRANSFORMS OF LOGARITHMS

The modification of the Laplace transform, introduced in Eq. (5), will be used to map invertibly functions $F(t)$ of time to functions of the complex frequency z. The functions are defined for $t>0$ and $\mathrm{Im}z>0$, respectively. Euler's second integral for the gamma function $\Gamma(y)$ implies $\mathcal{S}[t^x](z)=(i/z)^x\Gamma(1+x)$ if $x>-1$. Differentiating this identity n times for $x=0, n=0,1,2\ldots$, one arrives at the formula

$$\mathcal{S}[\ln^n(t)](z)=\sum_k \binom{n}{k}\Gamma_k \ln^{n-k}(i/z). \tag{A1}$$

Here $\binom{n}{k}=n!/[k!(n-k)!]$ and $\Gamma_k=d^k\Gamma(x=1)/dx^k$. One gets in particular $\Gamma_0=1$ and $\Gamma_1=-\gamma$, where γ is Euler's constant. If $\psi(y)$ denotes the digamma function, one can write $\Gamma'(y)=\Gamma(y)\psi(y)$. Iterating this formula, one can express Γ_k in terms of the first $(k-1)$ derivatives of $\psi(y)$ for $y=1$. The latter are given by the tabulated values of the zeta function $\zeta(k)$ [28]; for example, $\Gamma_2-\Gamma_1^2=\zeta(2)=\pi^2/6$. Implications of Eq. (A1) read with $n\geqslant 1, n_1\geqslant 1, n_2\geqslant 1$

$$\mathcal{S}[\ln^n(t)](z)-\mathcal{S}[\ln(t)]^n(z)=\frac{\pi^2}{12}n(n-1)\ln^{n-2}\left(\frac{i}{z}\right) + \sum_{k=3}^{n}\binom{n}{k}[\Gamma_k-\Gamma_1^k]\ln^{n-k}\left(\frac{i}{z}\right), \tag{A2}$$

$$\mathcal{S}[\ln^{n_1+n_2}(t)](z)-\mathcal{S}[\ln^{n_1}(t)](z)\mathcal{S}[\ln^{n_2}(t)](z) =(\pi^2/6)n_1n_2\ln^{n_1+n_2-2}(i/z)+\sum_{k=3}^{n_1+n_2}\left[\binom{n_1+n_2}{k}\Gamma_k -\sum_l\binom{n_1}{k-l}\binom{n_2}{l}\Gamma_{k-l}\Gamma_l\right]\ln^{n_1+n_2-k}(i/z). \tag{A3}$$

These formulas are needed for the evaluation of the function $f^{(2)}(z)$ in Eq. (25).

Specializing Eq. (A3) to $n_1=n$ and $n_2=1$ and using the definition of the linear operator $\mathcal{T}$ from Eq. (24), one gets

$$\mathcal{T}[\ln^n(t)](z)=(\pi^2/6)\left[n\ln^{n-1}(i/z)+\sum_{k=2}^{n}(n-k+1)\times\Gamma_{n,k}\ln^{(n-k)}(i/z)\right], \tag{A4}$$

where the coefficients are

$$\Gamma_{n,k}=\binom{n}{k}[\Gamma_{k+1}-\Gamma_k\Gamma_1]/[(\pi^2/6)(n-k+1)]. \tag{A5}$$

Let us construct polynomials $p_n(x)$ of degree $n=1,2,\ldots$ obeying Eqs. (26). Specializing Eq. (A4) to $n=1$ shows that one can choose $p_1(x)=x$. Assuming that the polynomials for degree $l<n$ are known, Eq. (A4) provides the formula for degree n

$$p_n(x)=x^n-\sum_{k=2}^{n}\Gamma_{n,k}p_{n+1-k}(x). \tag{A6}$$

Thus, the sequence of $p_n(x)$ can be constructed recursively in terms of the coefficients $\Gamma_{n,k}$. To derive Eqs. (29b)–(29d), one needs

$$p_2(x)=2.6160x+x^2, \tag{A7a}$$

$$p_3(x)=-2.1482x+3.9239x^2+x^3, \tag{A7b}$$

$$p_4(x)=-12.813x-4.2964x^2+5.2319x^3+x^4. \tag{A7c}$$

[1] U. Bengtzelius, W. Götze, and A. Sjölander, J. Phys. C **17**, 5915 (1984).
[2] V. I. Arnol'd, *Catastrophe Theory*, 3rd ed. (Springer, Berlin, 1992).
[3] W. Götze and L. Sjögren, Rep. Prog. Phys. **55**, 241 (1992).
[4] W. Kob, J. Phys.: Condens. Matter **11**, R85 (1999).
[5] W. Götze, J. Phys.: Condens. Matter **11**, A1 (1999).
[6] W. Götze and R. Haussmann, Z. Phys. B: Condens. Matter **72**, 403 (1988).
[7] W. Götze and L. Sjögren, J. Phys.: Condens. Matter **1**, 4203 (1989).
[8] L. Sjögren, J. Phys.: Condens. Matter **3**, 5023 (1991).
[9] S. Flach, W. Götze, and L. Sjögren, Z. Phys. B: Condens. Matter **87**, 29 (1992).
[10] I.C. Halalay, J. Phys.: Condens. Matter **8**, 6157 (1996).
[11] H. Eliasson, Phys. Rev. E **64**, 011802 (2001).
[12] M. Sperl, Diploma thesis, TU München, 2000.
[13] K. Binder and K. Schröder, Phys. Rev. B **14**, 2142 (1976).
[14] E. Bartsch, M. Antonietti, W. Schupp, and H. Sillescu, J. Chem. Phys. **97**, 3950 (1992).
[15] G. Hinze, D.D. Brace, S.D. Gottke, and M.D. Fayer, Phys. Rev. Lett. **84**, 2437 (2000).
[16] F. Mallamace, P. Gambadauro, N. Micali, P. Tartaglia, C. Liao, and S.-H. Chen, Phys. Rev. Lett. **84**, 5431 (2000).
[17] L. Fabbian, W. Götze, F. Sciortino, P. Tartaglia, and F. Thiery, Phys. Rev. E **59**, R1347 (1999); **60**, 2430 (1999).
[18] J. Bergenholtz and M. Fuchs, Phys. Rev. E **59**, 5706 (1999).
[19] K. Dawson, G. Foffi, M. Fuchs, W. Götze, F. Sciortino, M. Sperl, P. Tartaglia, T. Voigtmann, and E. Zaccarelli, Phys. Rev. E **63**, 011401 (2001).
[20] A.M. Puertas, M. Fuchs, and M.E. Cates, Phys. Rev. Lett. **88**, 098301 (2002).
[21] J.-P. Hansen and I. R. McDonald, *Theory of Simple Liquids*, 2nd ed. (Academic Press, London, 1986).
[22] W. Götze, in *Liquids, Freezing and Glass Transition*, Proceedings of the Les Houches Summer School of Theoretical Physics, Session LI, 1989, edited by J. P. Hansen, D. Levesque, and J. Zinn-Justin (North-Holland, Amsterdam, 1991), pp. 287–503.
[23] F. R. Gantmacher, *The Theory of Matrices*, (Chelsea Publishing, New York, 1974), Vol. II.
[24] W. Götze and L. Sjögren, J. Math. Anal. Appl. **195**, 230 (1995).
[25] W. Götze and L. Sjögren, J. Phys. C **17**, 5759 (1984).
[26] T. Franosch, M. Fuchs, W. Götze, M.R. Mayr, and A.P. Singh, Phys. Rev. E **55**, 7153 (1997).
[27] J. Bosse and U. Krieger, J. Phys. C **19**, L609 (1987).
[28] *Handbook of Mathematical Functions*, 7th ed., edited by M. Abramowitz and I. A. Stegun (Dover, New York, 1970).